

Article

A Holistic Approach for Energy Renovation of the Town Hall Building in a Typical Small City of Southern Italy

Margarita-Niki Assimakopoulos ¹, Dimitra Papadaki ¹, Francesco Tariello ^{2,*} and Giuseppe Peter Vanoli ²

¹ Group of Building Environmental Studies, Physics Department, University of Athens, 157 84 Athens, Greece; masim@phys.uoa.gr (M.-N.A.); dpapadaki@phys.uoa.gr (D.P.)

² Department of Medicine and Health Sciences, University of Molise, 86100 Campobasso, Italy; giuseppe.vanoli@unimol.it

* Correspondence: francesco.tariello@unimol.it; Tel.: +39-087-4404-957

Received: 4 August 2020; Accepted: 8 September 2020; Published: 17 September 2020



Abstract: The reduction of buildings energy demand represents one of the main goals in developed countries in order to achieve a sustainable future. In Italy a significant number of public administration offices are located in historical buildings, especially in small provincial towns. In this paper the analysis of the energy and environmental effects deriving from the plant renovation of the Palazzo San Giorgio, the building offices of the municipality of Campobasso (Southern Italy), is carried out. The simulation model of the building-plant system has been implemented with the TRNSYS software using data collected in the survey campaign. It has been calibrated on the basis of the billed electricity and gas consumption and then, further used to evaluate the reduction of the building primary energy demands and CO₂ emissions deriving from some non-invasive energy refurbishment measures: led lighting, thermostatic valves, cogeneration system and photovoltaic plant. The latter was considered in two variants: the first one provides a system completely integrated into the roof, the second one high efficiency non-integrated panels. The interventions have been evaluated both individually and combined. A primary energy saving of about 47% and a reduction in CO₂ emissions of 73% are obtained with the best combined renovation action.

Keywords: energy renovation; TRNSYS; energy and environmental analysis; dynamic simulation; photovoltaic plant; cogeneration; led lighting; thermostatic valves

1. Introduction

The world's energy demand has increased from 1971 to 2014 by 92% according to the International Energy Agency (IEA), with the building sector contributing to a large portion of this increase. In fact, the building sector attributed more than 30% of the global greenhouse gas emissions [1,2] and 40% of total energy consumption [3–6].

During the last decades the subjects of energy efficiency and indoor air quality of different types of buildings has gained the attention of the scientific community. The European Union is intensively trying to improve energy efficiency and increase the usage of renewable energy sources [7,8]. Several actions have been taken by the European Commission to reduce this energy consumption through two Energy Performance Building Directives: Directive 2002/91/EC and Directive 2010/31/EU shortly EPBD and EPBD recasting [9,10] with the Member States adopting actions to exploit energy savings from the building sector for both new and existing residential and non-residential buildings [11,12].

The targets established for 2030 by the latest Italian energy planning documents [13] provide for:

- a share of energy from RES in the gross final consumption of energy equal to 30% (22% in the transport sector);
- a reduction in primary energy consumption of 43%;
- a reduction in greenhouse gas emission with respect to 2005 in the sectors not included in the EU Emissions Trading System (such as transport, buildings, agriculture and waste) of 33%.

To achieve these results, a fundamental role is still attributed to the buildings sector; a wide decarbonization potential can derive from existing building not undergoing significant refurbishment, which constitute most of the total built environment. This potential can be better exploited by integrating energy efficiency aspect into policies and measures whose main purpose is something other than efficiency: structural renovation, earthquake-proofing, systems upgrading and refurbishment thereof [13].

In Italy the decree laying the groundwork and setting the new criteria to update and program performance standards for buildings in order to achieve the EU targets under the nearly-zero energy building policy was the Decree Law N.63 of 2013, converted into Law N.90 of 2013 [14]. In 2018 the increase in nearly zero-energy buildings reached the number of about 1400 units, most of which were newbuilds (90%) and used for residential purpose (85%). The refurbishment of over 130 mainly non-residential public buildings planned by the end of 2020 will further increase these numbers [13].

In Mediterranean countries, like Italy, most of the existing building stock is very old and those buildings are often considered as historic. In particular, in Italy about 18% of the buildings were built before 1919 and often they house public administrations or are public buildings (museum, library). Furthermore, as a general rule, the norms and programs to promote energy efficiency in Italy have always looked to public administration buildings as promotional models of energy efficiency and for these buildings stricter limits in terms of the building system characteristics or of time to achieve predetermined objectives have been set [14]. Nonetheless when dealing with their energy renovation, many constraints must be taken into consideration due to conservation regulations [15]. For these reasons in recent years, energy efficiency and thermal comfort in historic buildings have become high-interest topics. Preserving environmental and historic values of buildings is one of the important considerations, taking into account the historic value of buildings and following the law regulations within a multi-criteria approach [16]. Historically significant buildings are listed on local, national or international register providing certain degree of protection. Any physical alteration, to these important properties requires review and approval by the corresponding official body, with intense assessments in the early stages of the design phase of their retrofit plan [17].

Several researches have focused on improving the energy performance of historic buildings which represent the cultural heritage of many countries. Early studies and publications related to energy efficiency refurbishments of historic buildings began to emerge in the late 1970s and early 1980s. In a review research the analyses revealed that residential, religious and museum building types, especially from the last two centuries, were used as case studies. The case studies targeted towards the demonstration the feasibility of maintaining built heritage values of historic buildings while achieving significant improvements in their energy efficiency and thermal comfort [1]. In another research the analyses renovation focused on the energy performance of historic rural houses in three countries (Estonia, Finland, Sweden) in the Baltic Sea region. Energy renovation packages were calculated for different scenarios and different energy saving levels. The analysis showed that the improvement of building service systems and the energy source holds the largest energy saving potential. Moreover, that the energy savings depend on the targets, the typology of the building, the thermal transmittance of original structures, and the building service systems [16].

In another work the increasing value of a smart renovation of historic buildings and the sustainability of the energy solutions has been analyzed, verifying the importance of good rating within the early design process, in the energy performance sectors. The outcomes showed that better results can be reached in the environmental sustainability certification by means of added actions not strictly needed but allowed [18]. A case study in L'Aquila city center was proposed in another research work. That building, listed for its historical value, built in the 1930s, underwent seismic

and energy refurbishment. The solution proposed aimed at improving the energy efficiency of the structure, by using additional insulating layers, made of natural hemp material and pure cellulose flocks, on the walls and the ceiling of unheated spaces respectively [19]. Another work in the UK investigated the current local legislation and guidance relating to energy efficiency in heritage buildings and found that there is regional variation to energy retrofit in historic buildings between Scotland and the rest of the UK, according to conservation professionals leading to inconsistencies in energy retrofit application. Recommendations were made for a more consistent approach and for greater interdisciplinary cooperation to align conservation of energy with conservation of heritage [20]. A historic building in İzmir (Turkey) was studied in another work via a building energy simulation tool in order to determine the impacts of energy efficient performance after the retrofits. Building energy simulation tool was calibrated by comparing the measured and simulated indoor air temperatures and total energy consumptions. The retrofits which are not compatible with the cultural heritage values, were eliminated and the overall results showed that energy saving of more than 34% can be obtained without damaging the heritage value [21].

Another work investigated the refurbishment of a historical Italian building by integrating passive and active solutions to optimize the indoor thermal comfort and the energy performance using dynamic simulation of the building to predict the post-retrofit energy performance upgrading. The reported findings indicated that an integrated approach for the preservation and energy upgrading of buildings by improving their energy performance and environmental quality while protecting their heritage value is recommended [22]. In a study of twelve building types, typical of the historic building stock in Visby (Sweden), it was proved that cost-efficient methodologies for energy renovations are characterized by low renovation costs and additional insulation of building components with poor thermal properties. Furthermore, the environmental performance from the energy renovations was proved to be highly dependent on the chosen energy system boundary [23]. Another study focused on the PV installation in historic buildings and the ways to overcoming barriers related to this topic successfully. It proved to be that it is necessary to better understand the processes for both, historic preservation and solar PV project implementation, and to foster working with professionals in each sector to receive appropriate support and guidance [17]. Nonetheless, to the best of the author's knowledge not many studies have been focused on the integration of PV systems and holistic energy retrofit recommendations in historic buildings.

A study on a multi-story residential building in Sweden was conducted, showing that the optimum renovation of the building envelope offers 51% more energy savings for space heating when the building is in a northern climate zone compared to a southern zone. The study suggested that different renovation strategies for the building stock should also take into account the climatic zoning characteristics of the region. Nonetheless the broad range of studied climatic zones provides the opportunity to apply the obtained results to other climate zones to buildings with similar characteristics [24]. In Europe, after the national transposition of the European Directive 2002/91/EC on the building energy performance, some local governments have given indications on an appropriate balance between building conservation and measures to improve energy efficiency in historic buildings [18]. Therefore, based on all the above mentioned remarks, a case study of a historic building used as offices in Northern Italy is believed to provide essential contribution to the design and decision making process of the energy retrofit of historic buildings; taking into account studies which elaborate different function of buildings, different typologies, climatic conditions, different user's approach, market, and legislative regulations.

In this paper the energy and environmental benefits deriving from some renovation actions carried out on the technical plants of Palazzo San Giorgio, the historical building offices of the municipality of Campobasso (Southern Italy) are analyzed. Unlike what is conventionally done in an energy refurbishment, in this case, interventions relating to the building envelope have not been considered due to the type of building, but the ability to approach zero energy demands on the basis of an annual balance has been evaluated only by intervening on plants. A consolidate methodology has been applied (Section 2). It is based on an in-situ inspections campaign finalized to characterize

the building-plant system and its energy demands (Section 3) and on software model simulations (Section 4). The calibration of the model, carried out considering the billed energy consumption (Section 5), is necessary for the simulation of the renovation actions (Section 6) and is a prerequisite for obtaining reliable information on the possible advantages that can be achieved with respect to the target of reducing or even canceling energy requests and greenhouse gas emissions, about these results is discussed in the Section 7.

2. Applied Methodology

The methodology followed in the present work is depicted in the block diagram shown in Figure 1. The analysis starts with the energy diagnosis that consists of a deep characterization of the building-plant system, including: the building form and architecture, the envelope in terms of opaque and transparent components, the internal zones distribution based on the activities performed, the geometry of the structure and the technical equipment installed, also technological plants: heating, cooling, lighting, etc., loads management and energy demands in terms of gas and electricity consumption (from bills or measurement). The information collected are necessary for the second phase, in fact, these data are necessary to create the energy simulation model of the building-plant system and to reconstruct the monthly energy demand curves, joining the real data collected in a certain number of years. The simulation model allows a dynamic representation of the whole system behavior with a time-step that can be hourly or sub-hourly. It gives the opportunity to replicate activity during a certain period in which the analysis is carried out and to know strengths or weaknesses of the current situation. However, the reliability of the model must be verified with respect to the energy demands trends, elaborated in the aforementioned step (see Figure 1) [25,26].

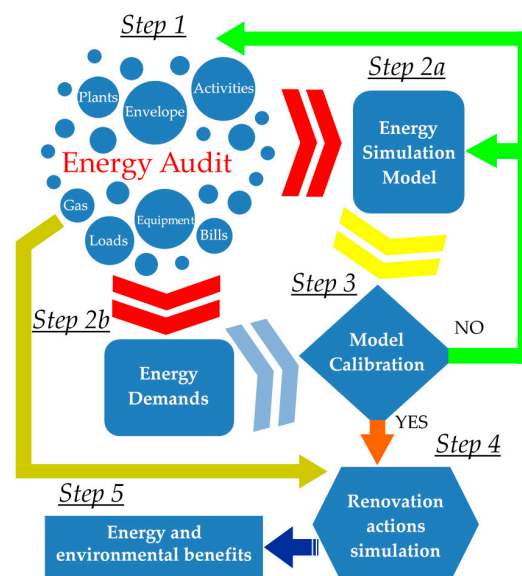


Figure 1. Scheme of the applied methodology.

A calibrated model is an essential tool to virtually implement renovation actions and to verify how modifications to the building envelope and to the technological systems affect the energy demands and greenhouse gas emissions in comparison to the state of fact reconstructed through the in-situ survey. The interventions selection should be supported by the information collected in the audit phase and by the simulation results. The last point of the analysis provides the evaluation of the energy and environmental benefits by means of the calculation of several significant indexes.

In particular to evaluate the effects of the interventions primary energy requests and CO₂ emissions are calculated and compared with those obtained from the simulation of the building-plant system in the current state of fact (SoF).

Two indexes are evaluated as comparison parameters: the percentage primary energy demand reduction ($\%E_pDR$) and the percentage CO₂ emissions reduction ($\%CO_2ER$), calculated according to the following equations:

$$\%E_pDR = \left(1 - \frac{E_p^{Act}}{E_p^{SoF}}\right) \quad (1)$$

$$\%CO_2ER = \left(1 - \frac{CO_2^{Act}}{CO_2^{SoF}}\right) \quad (2)$$

where the primary energy and the CO₂ emissions of the building-plant system at the state of fact, E_p^{SoF} and CO_2^{SoF} respectively, are evaluated considering the total electricity (lighting, device, auxiliaries), E_{el}^{SoF} , the electric grid efficiency (comprehensive of renewable energy contribution, distribution and transmission losses, $\eta_{el}^{EG} = 0.71$ [27,28]), gas consumption for heating (E_p^B) and the emission factor for electricity and gas consumption ($\alpha = 0.356$ kgCO₂/kWh_{el}, $\beta = 0.205$ kWh_p [27,28]), as specified below:

$$E_p^{SoF} = \frac{E_{el}^{SoF}}{\eta_{el}^{EG}} + E_p^{B,SoF} \quad (3)$$

$$CO_2^{SoF} = E_{el}^{SoF} \times \alpha + E_p^{B,SoF} \times \beta \quad (4)$$

while for the same contribution after renovation actions specific equations are reported in the following Section 7 case by case.

3. Description of Case Study and Field Data Collection

The case study chosen for the following analysis is Palazzo San Giorgio, a historical building in the city of Campobasso, that serves currently as the seat of the municipality of the town (Figure 2). Campobasso has 49,000 inhabitants and is located 700 m above sea level in the inner area of Southern Italy. It is characterized by a cold climate, in fact, it belongs to the climatic zone E (2346 Degrees Day).



Figure 2. The town hall of Campobasso: (a) North-East façade, (b) South-West façade, (c) top view of the building and (d) old view of the building.

An in-situ inspections campaign was performed to collect the data used to characterize the main elements of the building and its plants in the simulation software. Such information is necessary to build the simulation model and verify its reliability.

3.1. Building-Plant System Characterization

This subsection is dedicated to the description of the building and the technical plants serving it. During the survey phase the data listed below were collected independently in every single room:

- intended use;
- height between floors;
- number and type of radiators;
- additional heating systems (electric heaters);
- number and type of windows;
- number and type of lighting elements;
- number of working stations and their equipment.

In addition, the plans and the documentation of the plant room was recorded as well as the working hours and the 150 employees, (the details are given in Table 1).

Table 1. Working hour schedule.

Day	Working Hours
Monday—Wednesday—Friday	08:30–14:00
Tuesday—Thursday	08:30–14:00 and 15:00–18:00
Saturday	08:00–14:00 (only few people)
Sunday	Closed

3.1.1. Building Characteristics

Construction of Palazzo San Giorgio dates back to 1874–1876 (see Figure 2d), the building was built in the area once occupied by the Celestine convent, founded in 1209 by Pope Celestino V and destroyed by the devastating earthquake that struck Campobasso in 1805. The occupied area is about 1900 m². The building incorporates on the right side, looking the North-East façade, a church that is managed separately from the other rooms of the town hall. This façade has a large arched portico on the ground floor and two rows of windows above (see Figure 2a).

Over the years, due to the need of extra space, intermediate floors have been created. Therefore, in the town hall there are some rooms with 3 m height and others with 6 m height, and currently the building has a different number of floors in the different zones.

The South-West façade (see Figure 2b) shows two types of structures, the old one of the XIX century alternating with two steel and glass blocks of four floors, with a modern addition of a flat roof, introduced as an extension of the original building. The plan of the old structure has an E-shape (see Figure 2c) which, together with the two added blocks, delimits two internal cloisters.

The external and internal walls constitute the supporting structure of the building, they are made of mixed stones and concrete with a thickness of about 1 m, with an estimated thermal transmittance of 1.387 W/(m² K). The XIX century part of the building is covered by a pitched roof with brick tiles. The floor slabs of the lower floors are of various types, with a thermal transmittance of about 1 W/(m² K). In the case of the wooden structure a thermal transmittance of 1.818 W/(m² K) has been estimated for the brick and concrete slab, and also for the modern blocks of concrete slab floors.

Concerning the transparent structures, in the main part of the building new windows with wooden frame and double clear glazing with air gap are included, with estimated transmittance of approximately 2.3 W/(m² K). The windows around the internal cloisters have single glazing and aluminum frame, with transmittance of 5.68 W/(m² K). For the slightly darkened glass wall of the added blocks a transmittance value of 2.54 W/(m² K) has been considered.

3.1.2. The Air Conditioning System

The town hall is equipped with a heating plant operated on natural gas-fired boilers and radiators. The heat transfer fluid is heated up by two high efficiency 425.5 kW boilers with a rated efficiency equal to 92.6% (see Figure 3a). The supplied water temperature is adjusted according to the outdoor air temperature; a linear regulation curve is adopted: the supply water temperature is 80 °C when the outdoor air temperature is equal or lower than −4 °C, instead it is 60 °C with an outdoor temperature of 20 °C, over 20 °C the plant is switched off (see Figure 3b). The heating system operation is limited to the heating season from 15 October to 15 April, according to the Italian legislation. In addition, the daily operating hours are scheduled as reported in Table 2.

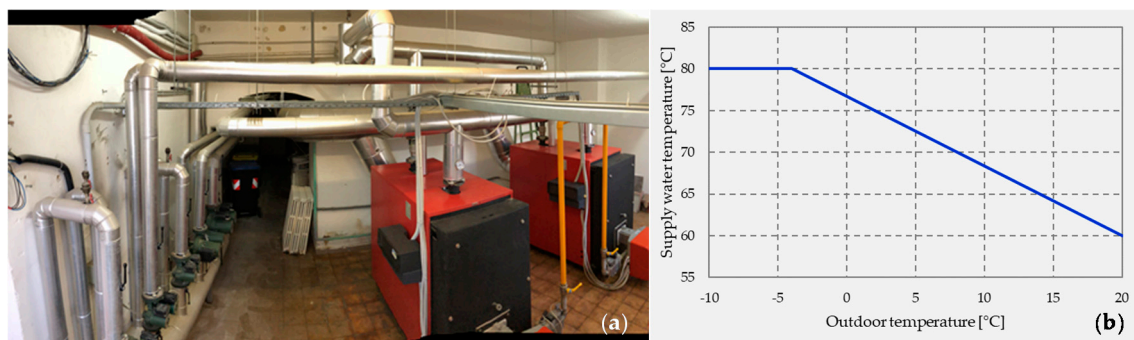


Figure 3. Plant room (a), boiler regulation curve (b) [29].

Table 2. Heating system daily operation periods.

Weekday	ON Period
Monday—Wednesday—Friday—Saturday	06:00–13:00
Tuesday—Thursday	06:00–12:30 and 14:30–18:30

The heat transfer fluid circulation is ensured by seven electric pumps with a total power of 5 kW. The radiators surveyed in the inspection phase are mainly of cast iron, but have different characteristics in terms of height, form, number of elements and columns; about 15 types have been identified (some examples are reported in Figure 4). In addition, in some rooms the presence and use of portable electric heaters has been verified, which are turned on by the occupants on particularly cold days. For these heaters, an average power of 1 kW is considered.



Figure 4. Several types of radiators [29].

3.1.3. The Lighting System and Office Electric Devices

The lighting plant showed a variety of lighting fixtures: wall lamps, spotlights, ceiling lights, chandeliers. Fourteen types of lamp have been detected, they are based on different technologies: neon, halogen, incandescent and led. Some examples are reported in Figure 5.



Figure 5. Several types of lamps [29].

Regarding the various electrical devices, with which each office is equipped, the prevailing ones are personal computer, monitor and printer for each desk as well as few common photocopiers.

3.2. Data Collection

Due to the high number of rooms in which the whole building is divided only the main cumulative data, representative for the survey campaign are reported in Table 3.

Table 3. Building main representative information.

Data	Values
Number of floors	3 + 3 mezzanine floors
Number of rooms (including offices, council room, user room, meeting room, toilets)	101
Number of working stations	144
Radiators number	143
Radiators estimated power (kW)	373.5
Supplementary electric heater number	63
Lamps number (including neon, halogen, incandescent and led)	366
Lamps estimated power (including neon, halogen, incandescent and led) (kW)	29.4
Number of printers	50
PC number	132
Estimated PC and printers power (kW)	39.4

Furthermore, bills related to electricity and gas consumption for three years were analyzed [29] obtaining the average monthly trend demand reported with red dots in Figures 6 and 7, respectively.

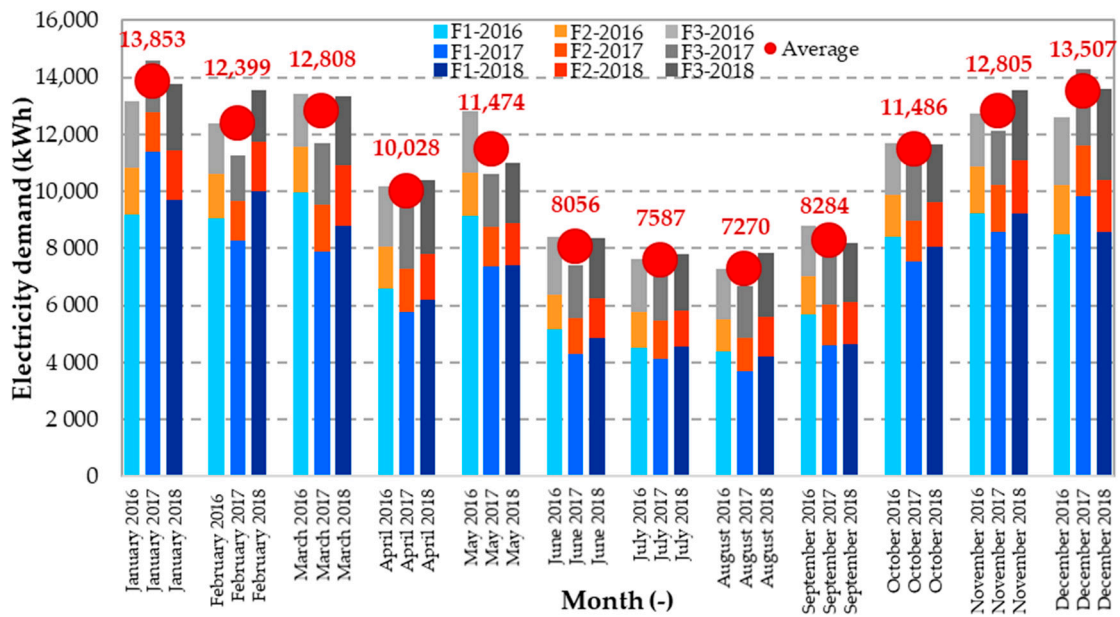


Figure 6. Monthly (bars) and average electricity demand (red circles) for the years 2016, 2017, 2018.

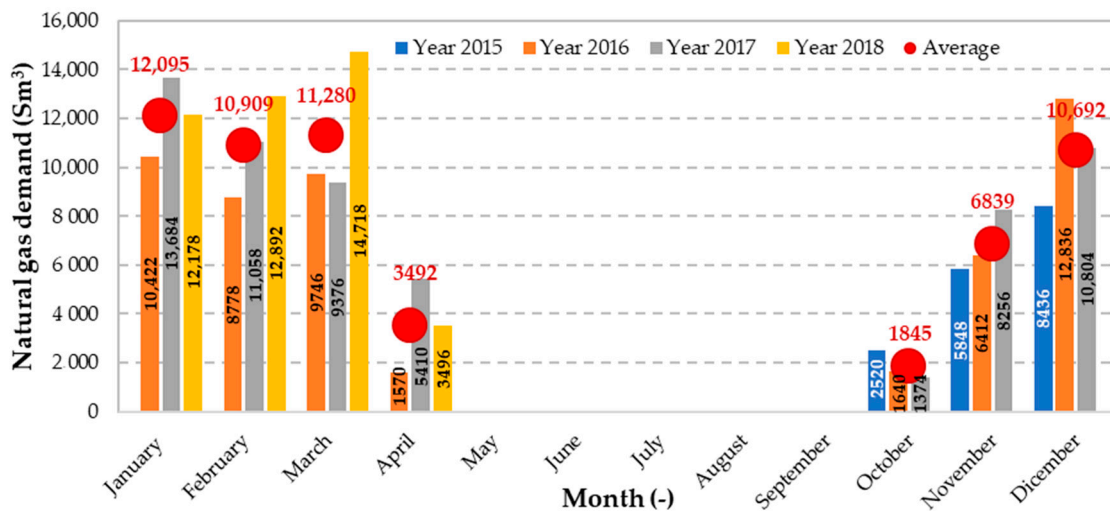


Figure 7. Monthly (bars) and average natural gas demand (red circles) for the years 2015 (from October to December) 2016, 2017, 2018 (until April).

The electricity consumption shows, in general, higher values during the winter period (from October to April), mainly due to the longer use of the lighting system and of the electrical heaters. In addition, the demand of electric energy is concentrated in the central hours of weekdays as demonstrated by the blue bars that correspond to the F1 period. F1, F2 and F3 are acronyms reported in the Italian bills to represent time slots for electricity billing, as detailed in Table 4.

Table 4. Time slots for electricity billing.

Time Slot Acronym	Period
F1	From 08:00 to 19:00 in the weekdays
F2	From 07:00 to 08:00 and from 19:00–23:00 in the weekdays, from 07:00 to 23:00 on Saturday
F3	The remaining period and holidays

For F2 and F3 periods more stable value are observed. Detailed information about the amounts billed electricity per time slots is reported in Table A1 of Appendix A. Natural gas consumption occurs only during the cold period of the year, especially from December to March. In the months of April and October the fuel volume taken from the grid is lower since the heating period is only 15 days and the outdoor temperatures are often higher than 20 °C in the central hours of the day.

4. Simulation Model

In the present research work simulations via TRNSYS (v.18.0, University of Wisconsin, Madison, WI, USA) modelling were conducted. TRNSYS has a modular structure and a user-friendly interface in which the elements are dragged and dropped from an organized list [30]. The elementary parts of the software, called *types*, need to be properly connected to each other for the realization of a complex system, which includes devices used for energy conversion (boiler, chiller, PV panels etc.), systems that transport the heat transfer fluids (pumps, ducts, fan, etc.) and further includes controls and plotting/saving tools.

Types are simplified representations of each component with which users interact, set parameters and connect inputs and outputs. The types are provided both directly in TRNSYS (standard library) and in external libraries such as the TESS library [31], each of them identified by a numeric or an alphanumeric code.

Type 56 is the type used for the building representation. Due to the high number of parameters required to characterize structures and loads and also due to the difficulty of defining the geometry, a supplementary tool of TRNSYS (TRNBuild) was used. To further simplify the building form insertion TRNBuild interfaces with the 3D design software SketchUp.

In order to model the town hall building, the 101 rooms identified in the survey phase were grouped into 43 thermal zones based on the intended use, location and layout. These zones were initially geometrically built with the 3D software (see Figure 8). Then, each zone was characterized according to the data collected for the envelope, the loads, and the occupancy. Electrical devices commonly used by occupants, such as PCs, were considered to be switched on based on the occupancy level of each thermal zone. With regard to the lighting system and the electric heaters, appropriate controls have been implemented to simulate the occupants' behavior as a function of solar radiation and internal temperature, respectively. Finally, the plant and the building were integrated in the whole system.

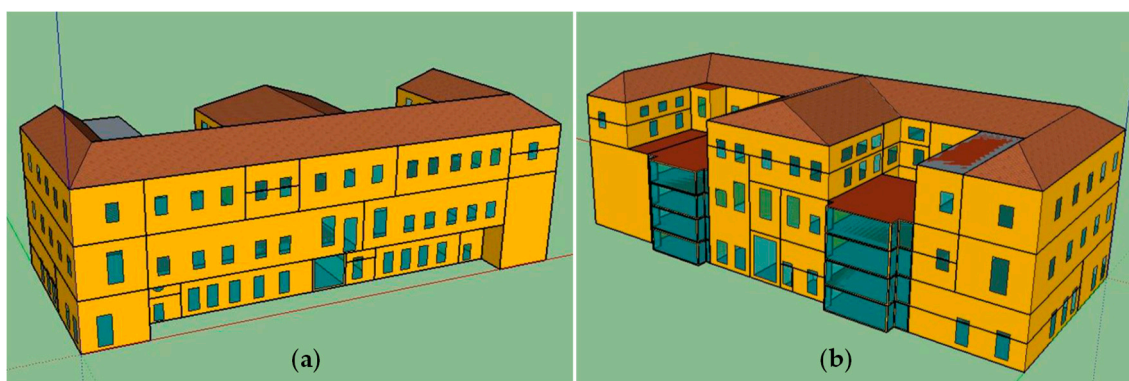


Figure 8. 3D sketch of Palazzo San Giorgio: north (a) and south view (b).

Regarding the heating system its main components and mathematical models are listed and briefly described below. The simple layout of the plant provides a boiler represented by the *type 751* of the TESS library whose simulation is based on a performance map expressed in terms of boiler (η^B) and combustion efficiencies (η_{comb}^B). If the boiler control is set to ON and there is a certain flow rate through the device (\dot{m}_f^B), on the base of the set-point temperature chosen ($T_{f,sp}^B$) for the supply temperature, the

return temperature ($T_{f,in}^B$), the maximum thermal power ($P_{th,max}^B$), the characteristics of the heated fluid (specific heat, $c_{p,f}$) and the performance map entered, the algorithm of the type calculates the effective supply fluid temperature ($T_{f,out}^B$), the fuel required (P_p^B), the exhaust (P_{exh}^B) and envelope (P_{env}^B) losses (P_{loss}^B) according to the following Equations (5)–(7) [31]:

$$T_{f,out}^B = T_{f,in}^B + PLR \times P_{th,max}^B / \dot{m}_f^B \times c_{p,f} \quad (5)$$

$$P_p^B = \dot{m}_f^B \times c_{p,f} (T_{f,out}^B - T_{f,in}^B) / \eta^B(PLR) \quad (6)$$

$$P_{loss}^B = \begin{cases} P_{exh}^B = P_p^B (1 - \eta_{comb}^B(PLR)) \\ P_{env}^B = P_p^B - P_{exh}^B \end{cases} \quad (7)$$

where η^B and η_{comb}^B are considered in table form as a function of $T_{f,in}^B$ and Partial Load Ratio (PLR) evaluated as in the following Equation (8) and limited to 0 or 1 if out of range included between them:

$$PLR = \dot{m}_f^B \times c_{p,f} (T_{f,sp}^B - T_{f,in}^B) / P_{th,max}^B \quad (8)$$

Hot water is conveyed to the radiators by a steel pipelines which are modeled using *type 31* of the standard library. The mass flow rate of the fluid in the pipe (\dot{m}_f^{Pipe}) is considered as a series of fully mixed subsequent cylinders that are at different temperatures ($T_{f,j}$) and whose mass is $M_{f,j}$. In each time step, that has a duration is expressed by θ_{ts} the output temperature ($T_{f,out}^{Pipe}$) and the environmental losses (P_{loss}^{Pipe}) are evaluated on the base of Equations (9) and (10), respectively [30]:

$$T_{f,out}^{Pipe} = \frac{1}{\dot{m}_f^{Pipe} \theta_{ts}} \left(\sum_{j=1}^{k-1} M_{f,j} T_{f,j} - a M_{f,k} T_{f,k} \right) \quad (9)$$

where $0 < a < 1$ and $\sum_{j=1}^{k-1} M_{f,j} - a M_{f,k} = \dot{m}_f^{Pipe} \theta_{ts}$.

$$P_{loss}^{Pipe} = \sum_{j=1}^k (UA)_j (T_j - T_e) \quad (10)$$

Finally, the radiators are represented with *type 1231* that refers to the specific characteristics of each terminal unit, often reported by manufacturers. In particular, the mathematical model is based on a power balance and manufacturers data. The thermal power supplied to the indoor air ($P_{th,air}^R$) and yielded by the fluid ($P_{th,f}^R$) are expressed respectively as shown in Equations (11) and (12) [31]:

$$P_{th,air}^R = F_a F_v C (T_S^R - T_{air})^n \quad (11)$$

$$P_{th,f}^R = \dot{m}_f^R \times c_{p,f} (T_{f,out}^R - T_{f,in}^R) \quad (12)$$

where $P_{th,air}^R$ corresponds to the supplied radiator thermal power in rated conditions corrected for the fluid velocity (F_v) and the altitude (F_a), while the surface temperature (T_S^R) is assumed equal to the average temperature between fluid input and output ($T_S^R = (T_{f,out}^R - T_{f,in}^R) / 2$). C and n are standard parameters typically reported in manufacturers datasheets for different terminal units.

5. Simulation Results and Comparison with Measured Data

Results of the building-plant system model, reproducing the town hall in the state of fact, are shown in Figures 9 and 10 in terms of electricity and gas consumption, respectively. In these figures the average energy demands (electricity and gas), derived from the bills of three years (see Section 3.2), are further reported in order to perform a comparison and assess the model calibration.

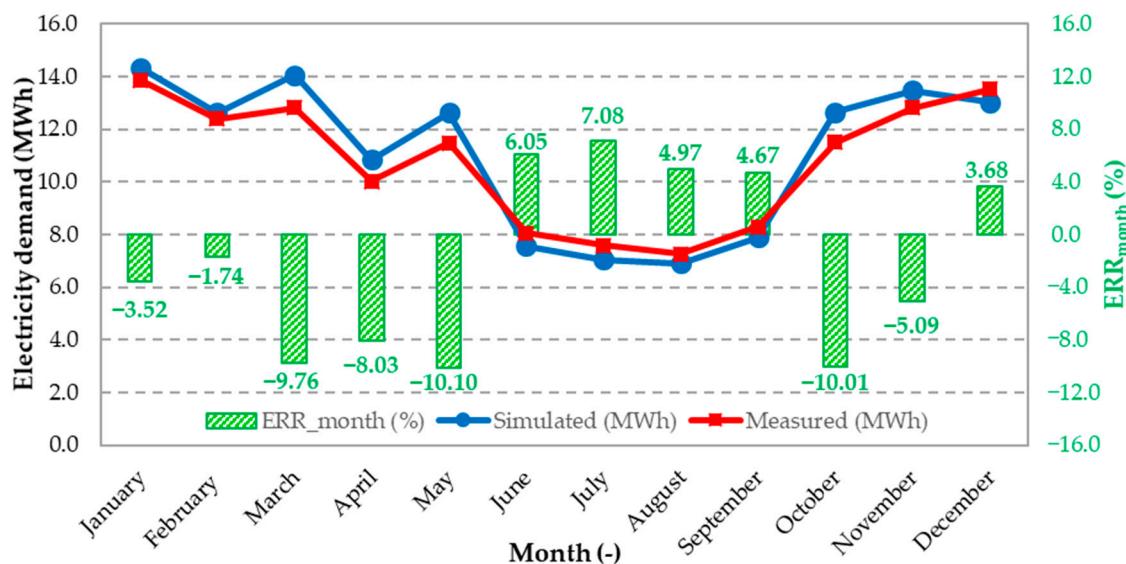


Figure 9. Simulated and billed (on average) monthly electricity demand in MWh and monthly errors (ERR_{month}) in percentage.

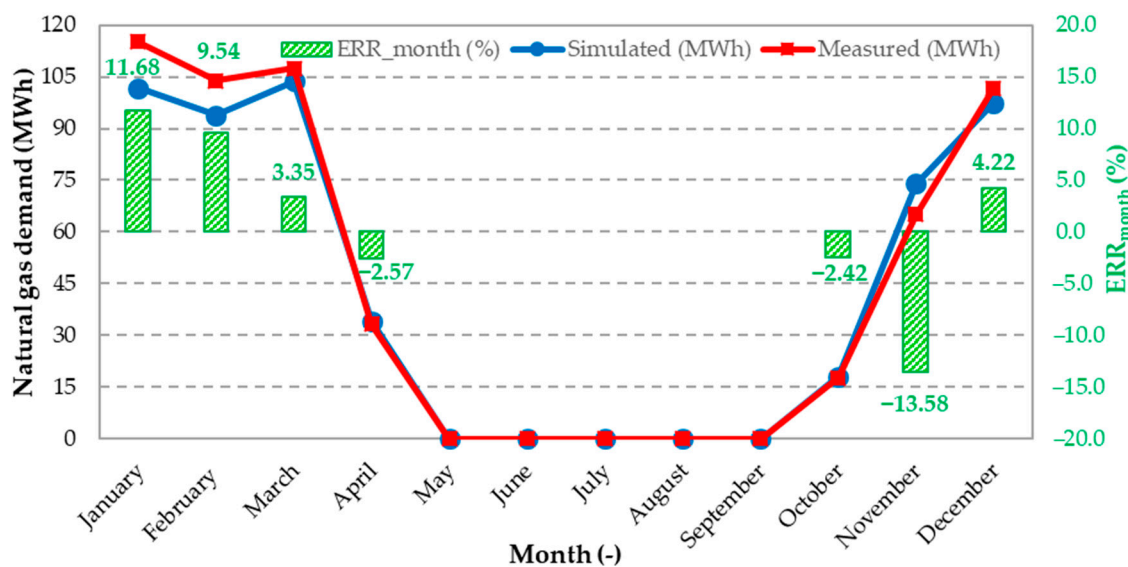


Figure 10. Simulated and billed (on average) monthly natural gas energy demand expressed in MWh and monthly errors (ERR_{month}) in percentage.

By analyzing the average measured demands for electricity and natural gas on an annual basis (129.6 and 544.1 MWh/y, respectively), a clear imbalance between the two request is observed and it is due to the high heating load. The climatic zone of Campobasso is characterized by severe winters which, associated with transmittance values of the building envelope far from those conventionally used in the so-called nZEB (nearly Zero Energy Building) buildings, determines a high demand for

natural gas despite being concentrated only in the winter period. The discontinuous operation of the plant and the absence of a regulation system also weighs negatively in this sense.

The simulated electric and gas requirements on monthly bases have been obtained summing the software outputs saved at each simulation step. The time-step has been selected to be equal to 5 min.

For both electricity and natural gas, monthly errors remain within the range $\pm 15\%$ according to M&V Guideline version 2 [25]. It is calculated as:

$$ERR_{month} = \frac{E_{month}^{meas} - E_{month}^{sim}}{E_{month}^{meas}} \times 100 \quad (13)$$

where E_{month}^{meas} and E_{month}^{sim} are the total energy demand of a month measured and simulated, respectively.

In regard to the electricity demand the worst error on a monthly basis was found to be -10% . In general, the simulation model lightly overestimates the effective electricity demand during the winter period, whereas in summer a slight underestimation is being observed. Natural gas requirements reproduction is slightly underestimated in the colder months (December–February), instead, it exceeds the recorded values in the intermediate months. Overall the proposed model can be considered well calibrated on the basis of the prescriptions reported in [4,26]. Table 5 lists an overview of the calibration indexes for both gas and electricity with the corresponding ranges of acceptability.

Table 5. Calibration indexes.

	ERR_{month}^{ave} (%)	MBE (%)	$Cv(RMSE)$ (%)
Electricity demand	-1.79	-2.63	6.87
Gas demand	3.88	1.46	9.60
Limits	± 10	± 5	± 10

The three indexes have been evaluated with the following equations. The average error, calculated with the monthly errors reported in Figures 9 and 10, is computed as:

$$ERR_{month}^{ave} = \frac{\sum ERR_{month}}{N_{month}} \quad (14)$$

where N_{month} is the number of months in which there is energy demand, it is 12 for electricity and 7 for gas.

The mean bias error (MBE) is assessed by subtracting the simulated energy request from the billed energy consumption of all the months and dividing the sum of these differences by the total demand measured in the considered year:

$$MBE = \frac{\sum_{month} (E_{month}^{meas} - E_{month}^{sim})}{\sum_{month} E_{month}^{meas}} \times 100 \quad (15)$$

Finally, the normalized measure of variability between measured and simulated data, here called coefficient of variation of the root-mean-squared error, $Cv(RMSE_{year})$, is expressed as:

$$Cv(RMSE_{year}) = \frac{RMSE_{year}}{E_{year}^{ave}} \times 100 \quad (16)$$

where the root mean square error, evaluated with monthly energy demands ($RMSE_{year}$), is obtained as:

$$RMSE_{year} = \sqrt{\frac{\sum_{month} (E_{month}^{meas} - E_{month}^{sim})^2}{N_{month}}} \quad (17)$$

while, the average monthly energy demand calculated on a year (E_{year}^{ave}) is:

$$E_{year}^{ave} = \frac{\sum_{month} E_{month}^{meas}}{N_{month}} \quad (18)$$

The “Whole Building Level Calibration with Monthly Data” approach [26] has proven that the simulation outputs are comparable with the average values of bills. In the following section several renovation actions will be simulated in order to evaluate their contribution on the reduction of energy requirements.

6. Simulated Renovation Actions

Significant restrictions can be encountered in a historic building when trying to intervene on the building envelope in order to reduce the heating and cooling load. Regarding the preservation of their architectural value and structures in their original forms, it is often not allowed to modify the elements of the envelope in any way. Further restrictions in the case of energy refurbishments can arise in the case of occupied buildings, for instance in buildings used as administrative offices, the renovation works will cause disturbance in the operation activity of the buildings and at the same time the offices occupancy will limit the renovation activities. This work intends to evaluate the potential primary energy savings achieved by introducing renovation actions that do not interfere with the building envelope. Therefore, interventions concerning the technical systems are taken into consideration and several feasibility limits are being analyzed and reported below.

The considered interventions include:

- the replacement and adaptation of the lighting system with led lamps;
- the adoption of thermostatic valves for temperature regulation;
- the installation of two natural gas powered cogenerators coupled with three thermal storage tanks;
- the introduction of a photovoltaic system;

In relation to this last action, a photovoltaic plant completely integrated into the roof was considered and alternatively it was also analyzed the installation of high efficiency photovoltaic panels, in order to evaluate the increase in primary energy savings and the emissions avoided in the case one intends to partially sacrifice the aesthetics of the building. Finally, the overall effects of the first three interventions considered together and combined with the two photovoltaic solutions are assessed. To make the description of the results easier, the above interventions will be referred to with the abbreviations shown in Table 6.

Table 6. Synthesis of the renovation actions and their abbreviations.

Action	Abbreviation
Replacement of existing lamps with led	Led
Adoption of thermostatic valves	T-V
Installation of cogenerators and storage tanks	Cog
Introduction of an integrated photovoltaic system	PV-I
Introduction of a high efficiency photovoltaic system	PV-HE
Combined renovation with PV-I	CR-PV-I
Combined renovation with PV-HE	CR-PV-HE

A multiplicity of further interventions has been considered but rejected due to the nature of the case study. Particularly the replacement of the existing boilers with biomass boilers (such as pellet boilers) has been considered as a potential action, however rejected due to space that was needed to the storage of the biomass to guarantee a certain period of operating autonomy without resorting daily supplies. The replacement of the existing boilers with an electric heat pump was another intervention that was considered. In this case two critical issues have been found, one related to the installation in

the plant room that does not have an appropriate connection with the outdoor; and the other linked to the terminal units (radiators) used in the rooms, which operate with high temperature water. The radiators also limit the use of condensing boilers, but, on the other hand, it is difficult to imagine their replacement with fan coils because it would create the need to redesign and re-realize the hot water distribution grid and the electricity network in order to ensure the correct flow rates to the terminals and also provide an electrical connection for the fan at the terminal installation point. The renovation of both grids was considered too invasive for the building under investigation, and so the aforementioned interventions were rejected.

As regards the first intervention, it was assumed that a power level per unit area of 4.5 W/m^2 corresponds to an efficient led lighting system. This value was chosen considering a luminous efficiency of 100 lm/W [32] and the illuminance for office rooms of 500 lx (according to UNI EN 12464-1 standard and [33]). In the case study the thermal zones compromise are composed by office rooms and common area (like corridors) therefore, a value of 4.5 W/m^2 seemed a good to characterize the specific load of the lighting system, according to [34,35]. Based on the data collected from the inspections, the power of the lighting systems has been adjusted to this value, significantly reducing the electrical load in most of the thermal zones.

The absence of an indoor temperature regulating system was noted in the town hall building and for this reason the installation of thermostatic valves in various thermal zones was considered with the aim of maintaining the internal temperature at around $20 \text{ }^\circ\text{C}$, avoiding the operation of the radiators in those thermal zones with higher temperatures.

The combined production of electricity and heat (cogeneration) can allow a better exploitation of the fuel compared to the separate production. As third action, the installation of 2 cogeneration units of $43 \text{ kW}_{\text{el}}$ and $90 \text{ kW}_{\text{th}}$ has been investigated [36]. Their main characteristics are shown in Table 7. These cogenerators, fueled with natural gas and equipped with internal combustion engine, are considered to function together with the existing boiler, due to their low capacity which prevents them to fully replace the heat generators. In order to operate these cogenerators primarily they are used to preheat the heat transfer fluid returning from the radiators. Additional, in order to increase their operating hours and the contribution to the thermal load, the two cogeneration units are coupled with 3 thermal storage tanks of about 2 m^3 each, thermally insulated with an 8 cm polyester fiber layer (thermal conductivity equal to 0.035 W/(m K)) [37]. An interface system with the electrical grid manages the surpluses and electrical deficits with respect to the user requests.

Table 7. Main rated characteristics of cogenerators [36].

Characteristics	Values
Net electrical base load power	43 kW
Thermal capacity	90 kW
Natural gas consumption	$14.8 \text{ m}^3/\text{h}$
Exhaust gas flow rate	188 kg/h
Thermal power recovery from exhaust	27 kW
Electrical efficiency	30%
Thermal efficiency	63%
Generator efficiency	91.2%
Engine type	8V—Otto cycle

The first intervention considering the photovoltaic plant (PV-I) is an integrated solution. It consists of roofing elements that have the shape of tiles and contain photovoltaic cells. Therefore, this choice has a low visual impact, [38], limiting the roof modification and preserving the exterior aspects and architectural values of a historical building. Such a system needs a surface of about 11 m^2 per kW of peak power. For the case study under consideration by placing the photovoltaic system on the roof flaps facing south-east and south-west, as shown in the simplified sketch of Figure 11a a total power of $47 \text{ kW}_{\text{pp}}$ is reached. Further data concerning these photovoltaic elements are listed in Table 8.

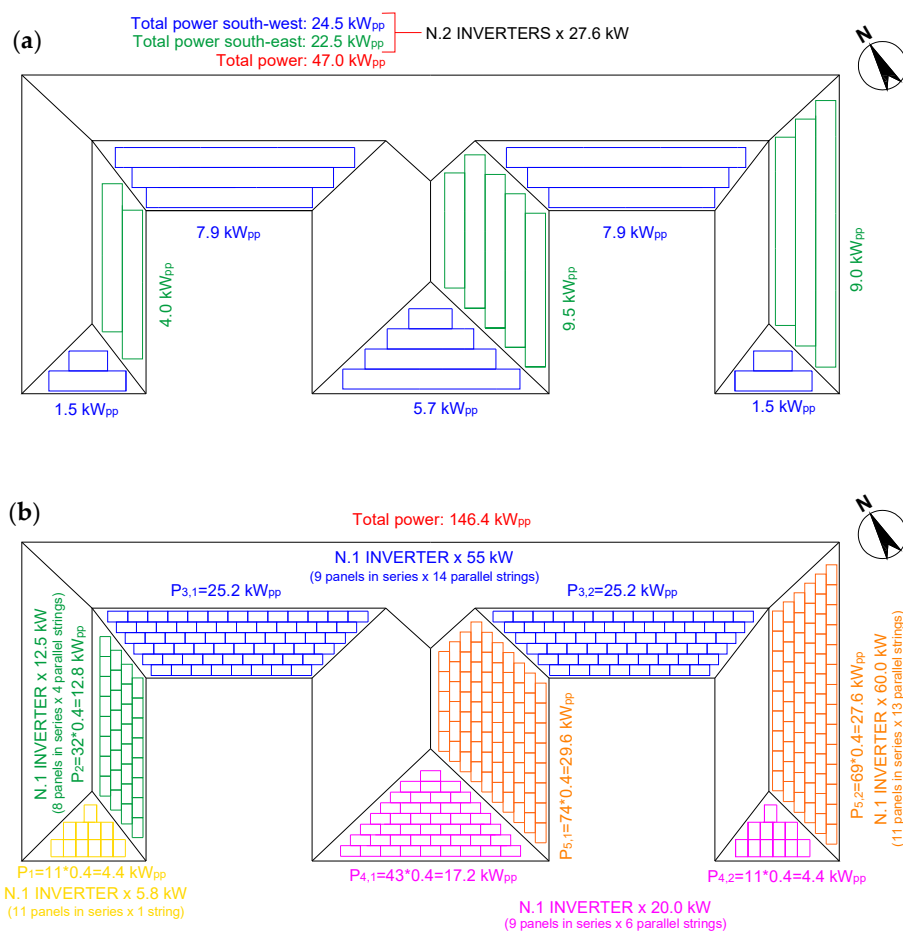


Figure 11. Simplified scheme of the PV-I (a) and PV-HE (b).

Table 8. Main rated characteristics of integrated photovoltaic elements [38].

Characteristics	Values
Rated power	45 W _{pp}
Rated voltage	5.76 V
Rated current	7.81 A
Open circuit voltage	7.51 V
Short circuit current	8.09 A
Temperature coefficient of short circuit current	4.28 mA/°C
Temperature coefficient of open circuit voltage	−0.026 V/°C
NOCT *	41.73 °C
length	2.25 m
width	16.7 cm
Number of cells	12

* Nominal Operating Cell Temperature.

Two 27.6 kW inverters, one for the photovoltaic elements facing south-east and one for those of the south-west roof flaps, with efficiency equal to 98.2% [39], are used for the DC to AC conversion and the power flows management to or from the distribution grid.

The second solution for the photovoltaic system considers standard high efficiency panels with a peak power of 400 W_{pp} each to be mounted coplanar to the roof [40]. Their main features are reported in Table 9. Also, in this second case the roof flaps facing south-east and south-west are covered by the photovoltaic system. A total of 366 panels (overall power 146.4 kW_{pp}) can potentially be installed on the base of the simplified scheme of Figure 11b.

Table 9. Main rated characteristics of high efficiency photovoltaic panels [40].

Characteristics	Values
Rated power	400 W _{pp}
Rated voltage	65.8 V
Rated current	6.08 A
Open circuit voltage	75.6 V
Short circuit current	6.58 A
Temperature coefficient of short circuit current	4.28 mA/°C
Temperature coefficient of open circuit voltage	−176.8 mV/°C
NOCT *	45.0 °C
length	1.69 m
width	1.05 cm
Number of cells	104

* Nominal Operating Cell Temperature.

The panels are divided into five groups, each connected to an inverter, with some further details about the electric configuration (panels in series and strings in parallel) shown in Figure 11b. The nominal power of the five inverters and their maximum efficiency are listed in Table 10. For both PV-I and PV-HE a total loss coefficient of 7% is assumed to consider the issues of mismatching, ohmic losses, dirtying etc.

Table 10. Rated characteristics of inverters used in action PV-HE.

	Inverter 1 [41]	Inverter 2 [42]	Inverter 3 [43]	Inverter 4 [39]	Inverter 5 [44]
Nominal power (kW)	5.8	12.5	55.0	20.0	60.0
Maximum efficiency (%)	98.0	97.8	96.3	98.2	98.5

Concerning the last two interventions (CR-PV-I and CR-PV-HE) they are a combination of the first three actions listed, combined with the two photovoltaic solutions.

7. Results of Renovation and Comparison with Actual Situation from an Energy, Environmental Point of View

In this subsection the results of the simulation for the building-plant system after each renovation action are analyzed and compared with the simulated results of the case study at the state of fact (SoF). The comparison is carried out considering the monthly primary energy demands, taking into account both electricity and gas consumption. In addition, the CO₂ emissions associated to electricity production and those related to the gas combustion are also evaluated and compared.

7.1. Action 1: Led Lamps

Regarding the lighting system, the primary energy demand of the renovated system (E_p^{Led}) is evaluated similarly to that of the SoF case (Equation (3)), but with different values of the electricity and gas demand (E_{el}^{Led} , and $E_p^{B,Led}$ respectively), in particular it is:

$$E_p^{Led} = \frac{E_{el}^{Led}}{\eta_{EG}} + E_p^{B,Led} \quad (19)$$

Figure 12a shows a slight reduction in the total primary energy demand (blue bars with respect to green bars), in fact, the advantage derives only from the reduction of electricity request. The primary energy due to lighting is on average the 3% of the total primary energy demand during the winter months in the SoF and about 8% during the months in which the heating system is off.

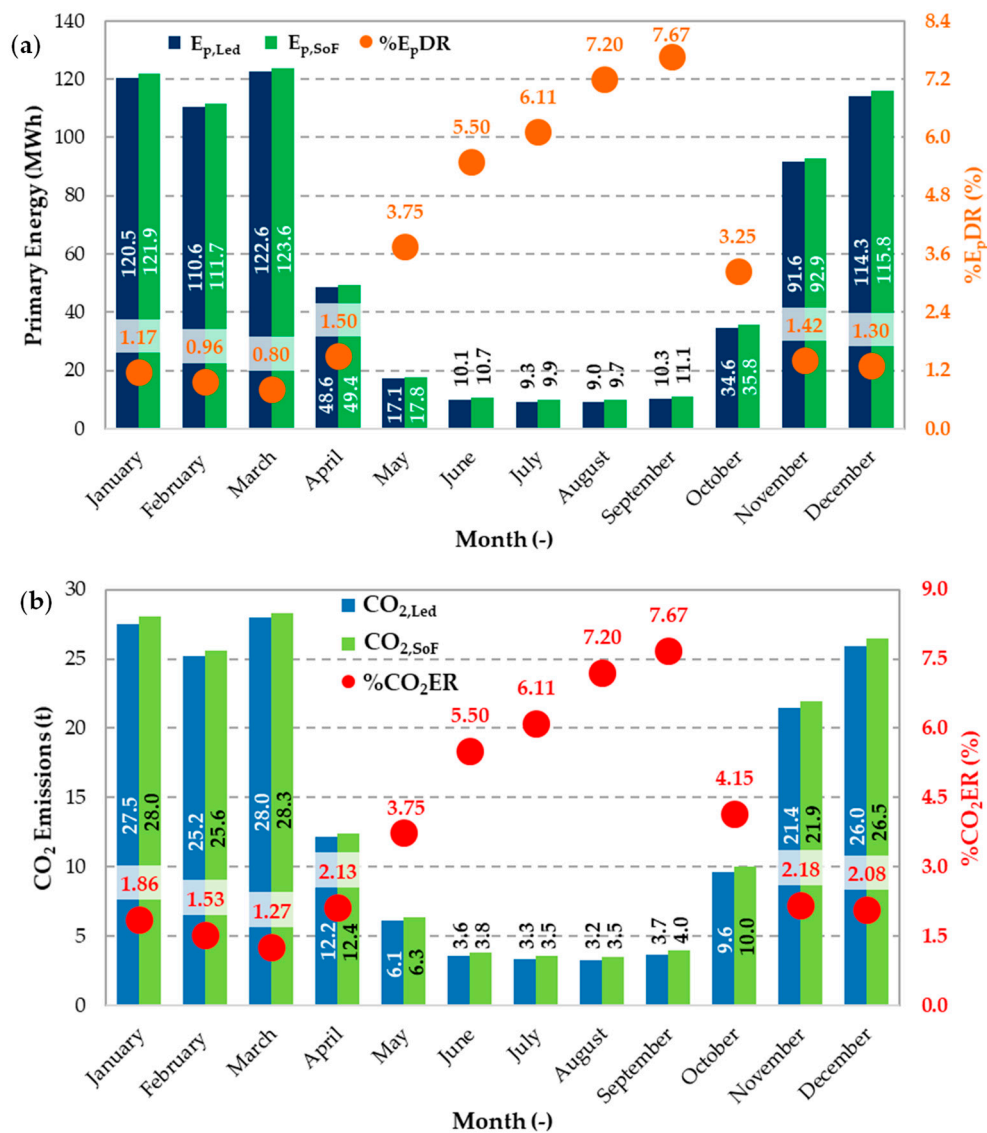


Figure 12. (a) Primary energy comparison (blue and green bars) and percentage primary energy demand reduction (orange circles), (b) CO₂ emissions (light blue and green bars) end percentage reduction (red circles) between Led lamps and SoF on a monthly basis.

In this last period the total primary energy drops drastically because the heating system is off and the monthly %E_pDR increases slightly since natural daylight hours increase and the lighting system is turned off. In addition, during the winter months the thermal energy for heating and consequently the associated primary energy increase because of the reduction thermal contribution of the lamps.

In terms of CO₂ emissions, the tons of greenhouse gas (GHG) after led lighting introduction are evaluated using Equation (20) that is similar to Equation (4):

$$CO_2^{Led} = E_{el}^{Led} \times \alpha + E_p^{B,Led} \times \beta \quad (20)$$

in which the electricity (E_{el}^{Led}) and primary energy demand of the boiler ($E_p^{B,Led}$) are those of the case considered (Led). The reduction in the electricity demand increase the benefits with respect to the primary energy reduction in the winter months, %CO₂ER values (Figure 12b) are higher than %E_pDR. On the base of emission factors (α and β) a reduction in electricity reduction is more beneficial than in gas consumption. During the summer months %CO₂ER and %E_pDR values correspond because are only linked to electricity and α is considered constant.

7.2. Action 2: Thermostatic Valves

The second renovation action considered (T-V) has effects only on the primary energy requirements and CO₂ emissions of winter months when the heating system is active, affecting only the heating load, as shown by the percentage indexes and the bars in Figure 13a,b. The percentage primary energy demand and CO₂ reduction have been evaluated with Equations (1) and (2) in which E_p^{Act} and CO_2^{Act} are replaced by E_p^{Led} and CO_2^{Led} , respectively:

$$E_p^{Led} = \frac{E_{el}^{T-V}}{\eta_{el}^{EG}} + E_p^{B,T-V} \quad (21)$$

$$CO_2^{Led} = E_{el}^{T-V} \times \alpha + E_p^{B,T-V} \times \beta \quad (22)$$

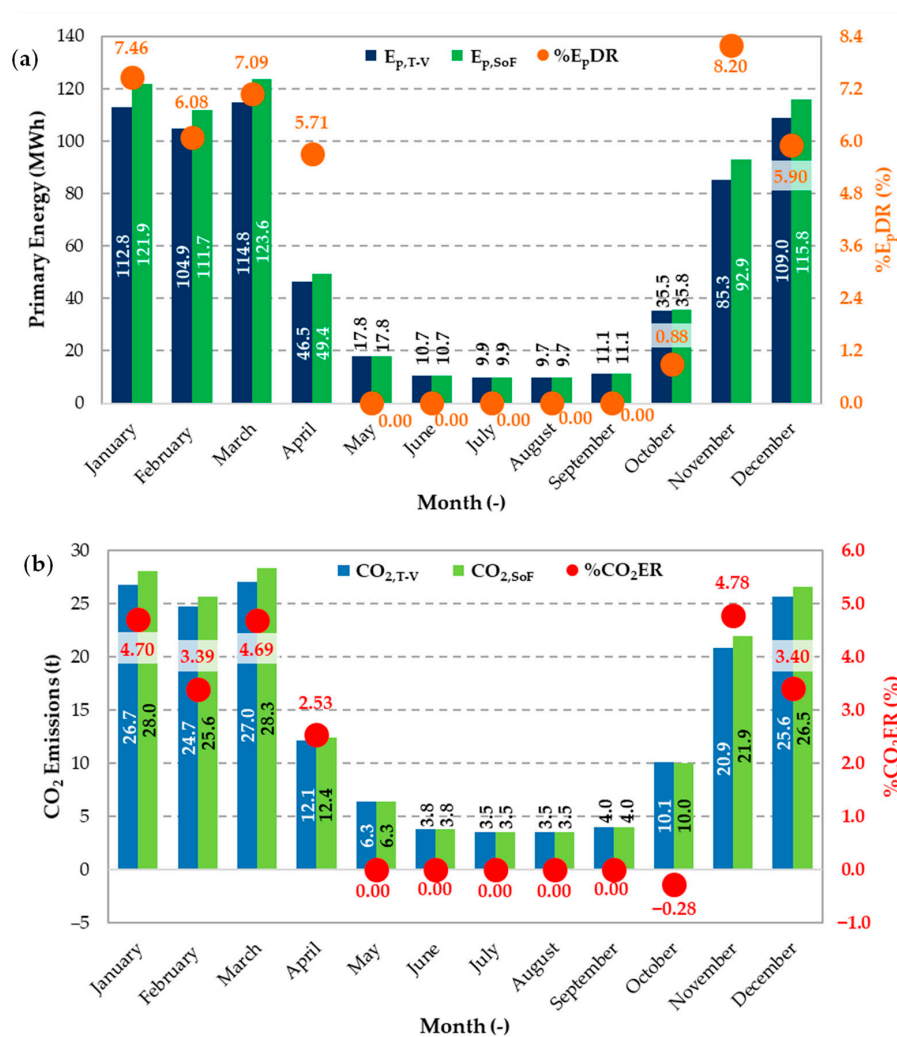


Figure 13. (a) Primary energy comparison (blue and green bars) and percentage primary energy demand reduction (orange circles), (b) CO₂ emissions (light blue and green bars) end percentage reduction (red circles) between Thermostatic Valves (T-V) and SoF on a monthly basis.

In this case the electric energy of the user (E_{el}^{T-V}) and the primary energy of the boiler ($E_p^{B,T-V}$) are different from those obtained in the state of fact. In particular, the decrease of the boilers primary energy (about 12% with respect to SoF) is partially compensated by an increase (10% with respect to SoF) of the electric load. It is due to a longer use of the electric heaters in those rooms where the heat supplied by the radiators is not sufficient and a lower temperature of the thermal zones close to the

colder ones amplify the problem. Unlike the previous case, the reduction of CO₂ emissions is less marked than the percentage decrease in primary energy, the reason is also in this case related to the emission factors; in terms of CO₂ emissions it is more beneficial the reduction of the electricity demand than the natural gas request.

7.3. Action 3: Cogenerators

The installation of the two cogenerators, as well as the thermostatic valves, changes the primary energy requirements and CO₂ emissions only during the months in which the heating system is switched on (see Figure 14a,b).

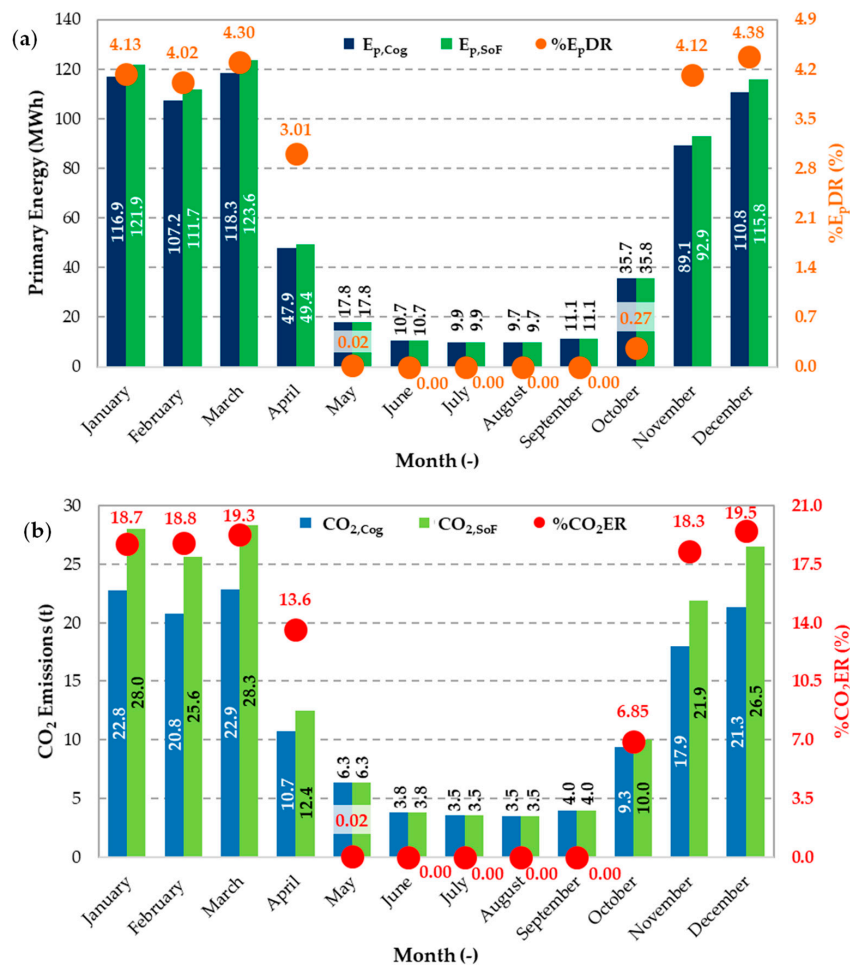


Figure 14. (a) Primary energy comparison (blue and green bars) and percentage primary energy demand reduction (orange circles), (b) CO₂ emissions (light blue and green bars) end percentage reduction (red circles) between cogenerators and SoF on a monthly basis.

A substantial difference appears in the evaluation of the primary energy demands (E_p^{Cog}) and CO₂ emissions (CO_2^{Cog}) with respect to what was done previously. The electricity fed into the grid (power surplus, $E_{el,tg}^{Cog}$) is considered as a credit for the investigated building-plant system and therefore it is subtracted from the total one. The primary energy deriving from the natural gas burned in the CHP operation (E_p^{CHP}), instead, is added:

$$E_p^{Cog} = \frac{E_{el,fg}^{Cog} - E_{el,tg}^{Cog}}{\eta_{el}^{EG}} + E_p^{B,Cog} + E_p^{CHP} \quad (23)$$

CO₂ emissions are assessed with the same criteria:

$$CO_2^{Cog} = \left(E_{el,fg}^{Cog} - E_{el,tg}^{Cog} \right) \times \alpha + \left(E_p^{B,Cog} + E_p^{CHP} \right) \times \beta \quad (24)$$

In the town hall, thermal energy cannot be used during summer months, for instance to activate a thermal-driven heat pump, therefore the advantage deriving from the simultaneous production of electrical and thermal energy is limited to a part of the year. The primary energy saving is less important than that achieved with the thermostatic valves, just over 4% reduction in the colder months. Three main reasons determine this situation. The first one is the low contribution of the cogenerators, which have a small capacity, limited by the installation constrains reported above. A second limiting factor for the energy supplied by the cogenerators is the few operating hours of the heating system which is coordinated with the building occupancy. The third reason is the high efficiency of the national electric system that increases year by year under the effect of the intensive renewable energy exploitation.

The higher percentages in the emission reduction with respect to % E_pDR is due to the beneficial effects of the electricity production that is partially used on-site ($E_{el,os}^{CHP}$) and partially supplied into the distribution grid ($E_{el,tg}^{Cog}$). The power flows to and from the grid and the CHP electricity used on-site are graphically reported by the histogram of Figure 15 on a monthly basis.

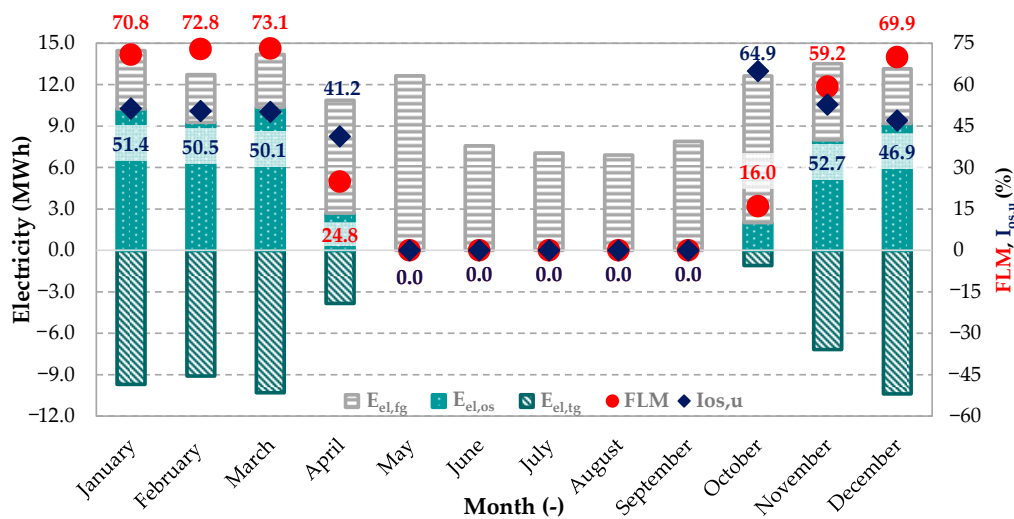


Figure 15. Electricity balance considering CHP electricity production, Fraction of Load Met (FLM , solid red circles) and index of on-site use ($I_{os,u}$, solid blue rhombus). In each stack: the dark green textured bars represent the electric energy fed into the grid ($E_{el,tg}$), the light green textured bars the electric energy used on-site ($E_{el,os}$), the gray textured bars the electricity taken the grid ($E_{el,fg}$).

The fraction of load met index (FLM), representing the percentage fraction of the electric load covered with the CHP electricity:

$$FLM = \frac{E_{el,os}^{CHP}}{E_{el}^{Cog}} \times 100 \quad (25)$$

where E_{el}^{Cog} is the total electric load in the case cogenerators were installed, showing for the months of January, February and March values higher than 70% and slightly lower in the months of November and December. At the same time the on-site use Index, evaluating the fraction of the electricity generated by the CHP used on-site is:

$$I_{os,u} = \frac{E_{el,os}^{CHP}}{E_{el}^{CHP}} \times 100 \quad (26)$$

and reveals that only half of the total electricity of the CHP units (E_{el}^{CHP}) is used by the user. During the summer period both FLM and $I_{os,u}$ are equal to zero because the cogenerators are turned off.

7.4. Action 4 and 5: Integrated and High Efficiency Photovoltaic System

Renovation actions 4 and 5, which consider PV plants are analyzed following the same approach. The production of electricity takes place all year round, therefore, unlike the previous cases, the requests for primary energy ($E_p^{PV-I/HE}$) and CO₂ emissions ($CO_2^{PV-I/HE}$) vary compared to those simulated in SoF every month, as highlighted in Figures 16 and 17. The following equations show that the contribution of the boilers to $E_p^{PV-I/HE}$ and $CO_2^{PV-I/HE}$ are the same of SoF:

$$E_p^{PV-I/HE} = \frac{E_{el,fg}^{PV-I/HE} - E_{el,tg}^{PV-I/HE}}{\eta_{el}^{EG}} + E_p^{B,SoF} \tag{27}$$

$$CO_2^{PV-I/HE} = \left(E_{el,fg}^{PV-I/HE} - E_{el,tg}^{PV-I/HE} \right) \cdot \alpha + E_p^{B,SoF} \cdot \beta \tag{28}$$

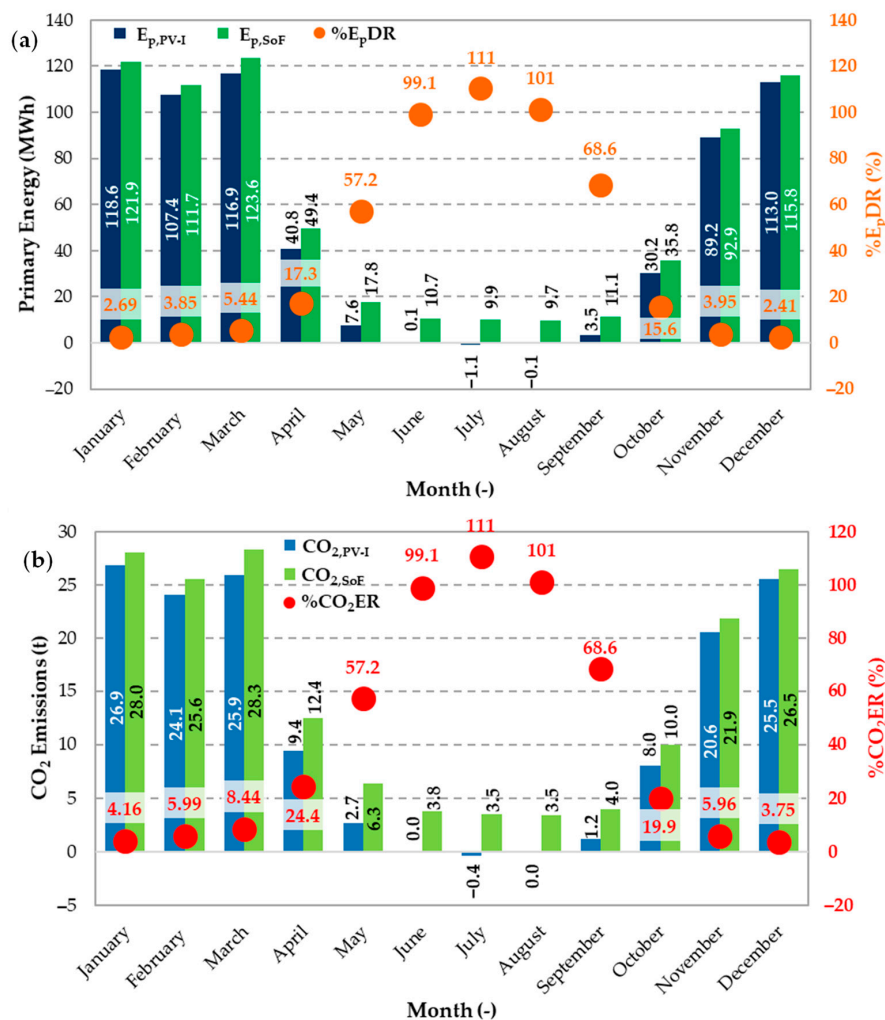


Figure 16. (a) Primary energy comparison (blue and green bars) and percentage primary energy demand reduction (orange circles), (b) CO₂ emissions (light blue and green bars) end percentage reduction (red circles) between PV-I and SoF on a monthly basis.

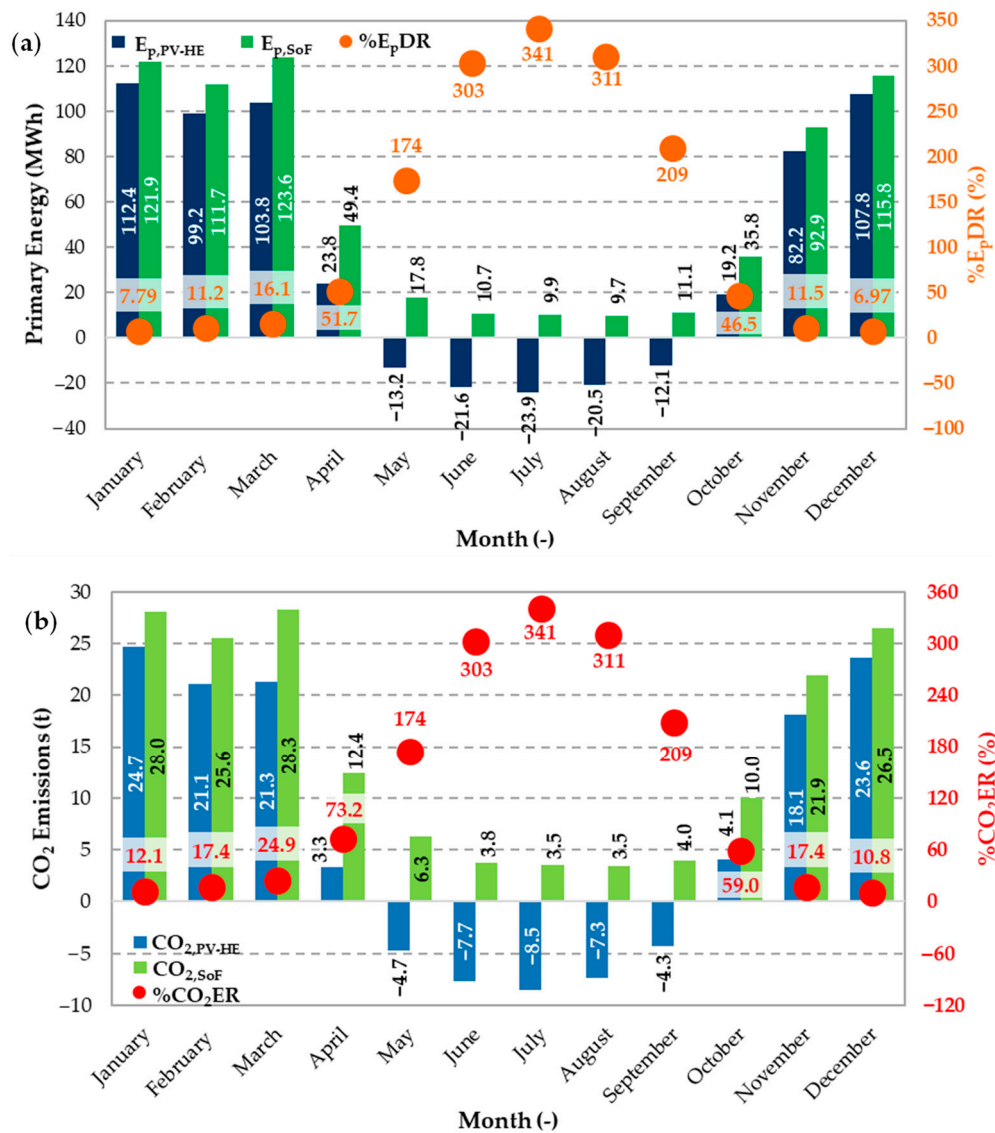


Figure 17. (a) Primary energy comparison (blue and green bars) and percentage primary energy demand reduction (orange circles), (b) CO₂ emissions (light blue and green bars) and percentage CO₂ emissions reduction (red circles) between PV-HE and SoF on a monthly basis.

The use of an integrated photovoltaic system (PV-I) reduces primary energy demands in the winter months, with a reduction below 6% (Figure 16a), due to the high energy contribution of the boilers. During the summer months, electricity production from the photovoltaic plant increases due to the higher level of solar radiation, instead, the term linked to the heating ($E_p^{B,SoF}$) disappears and it is observed that in July and August E_p^{PV-I} it becomes negative. The latter situation represents the condition in which the electricity transferred to the grid is greater than that taken from it, in fact, % E_pDR is greater than 100%. In this regard, one can also compare the dark green oblique striped and the gray checkered bars for PV-I in the months of August and July in Figure 18.

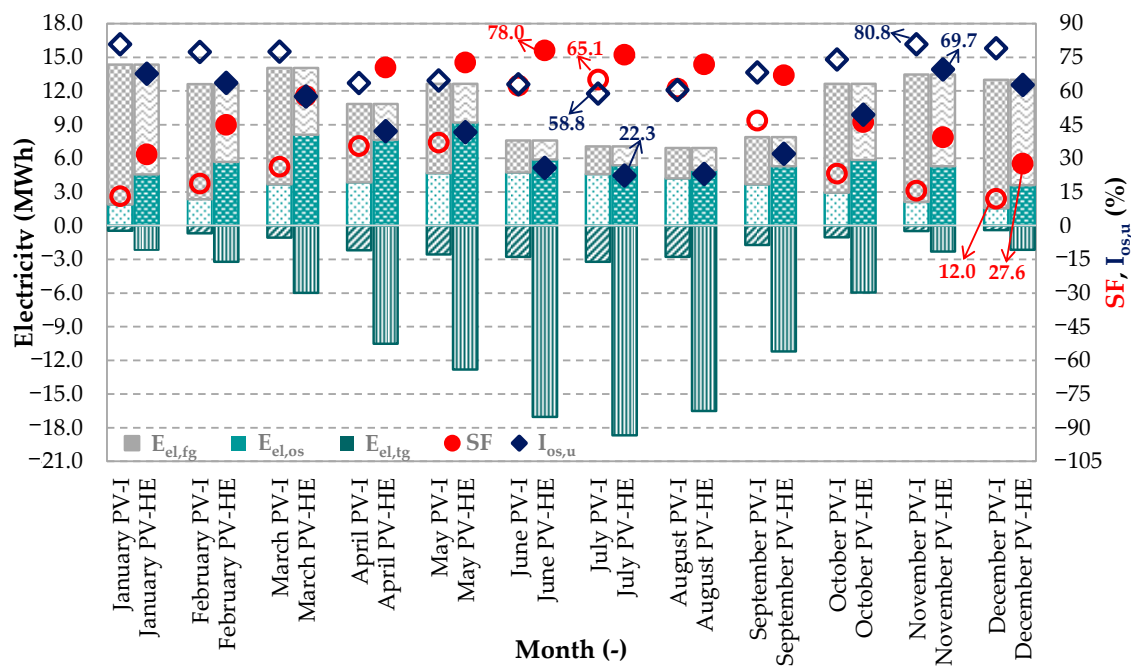


Figure 18. Electricity balance considering PV electricity production, Solar Fraction (SF) and index of on-site use ($I_{os,u}$). In each block of bars (one per month): the first stack refers to PV-I, the second one to PV-HE, while in each stack: the dark green textured bars represent the electric energy fed into the grid ($E_{el,tg}$), the light green textured bars the electric energy used on-site ($E_{el,os}$), the gray textured bars the electricity taken the grid ($E_{el,tg}$). Instead, the solid symbols (circle and rhombus) refer to PV-HE while the empty ones to PV-I.

Figure 18 shows the electrical balance in the form of a histogram in the case of the two photovoltaic systems. In addition, the solar fraction (SF) and the on-site use index of the electricity produced ($I_{os,u}$) are represented with red circles and dark blue rhombuses, respectively. The solar fraction is similar to FLM representing the ratio between the solar electricity used directly by the user and the total photovoltaic production. $I_{os,u}$, instead, compares the solar electricity used on-site to the total production. The share of electricity used on-site with respect to the production is in the range 74–81% from October to March when the adopted measure is PV-I, but the contribution to the load is limited and the SF is low. In the summer months the photovoltaic electricity fed into the grid exceed the on-site exploitation especially for PV-HE, in this case SF increases, but $I_{os,u}$ decreases. Monthly detailed values of these two indexes are listed in Tables A2 and A3 of Appendix A.

Regarding CO_2 emissions (Figure 16b), it is noted that in the winter months there is a percentage advantage greater than the reduction of primary energy, due to the values of the emission factors (α and β). In the summer period when there is only demand for electricity, the $\%E_pDR$ coincides with the $\%CO_2ER$.

In the case of the intervention 5 (PV-HE) the higher peak power of the panels and their higher conversion efficiency determines that $\%E_pDR$ reaches 16% in March (Figure 17a) and in the summer months there is a huge surplus of electricity transferred to the national electric grid (see the dark green vertical striped bars in Figure 18). For this reason, E_p^{PV-HE} is negative, representing a primary energy saving greater than 300% between June and August.

For the PV-HE case the same observations were made regarding CO_2 emissions of the PV-I case, however, the benefits achieved are significantly greater (Figure 17b).

7.5. Action 6 and 7: Combined Action with Integrated and High Efficiency Photovoltaic System

The last two cases analyzed in this subsection contemplate a combined renovation of the plants which involves the use of thermostatic valves, led lamps, 2 cogenerators, 3 tanks and alternatively the integrated photovoltaic system and the high efficiency photovoltaic system.

In both CR-PV-I and CR-PV-HE the primary energy demand and CO₂ emissions can be evaluated as:

$$E_p^{CR-PV-I/HE} = \frac{E_{el,fg}^{CR-PV-I/HE} - E_{el,tg}^{CR-PV-I/HE}}{\eta_{el}^{EG}} + E_p^{B,CR-PV-I/HE} + E_p^{CHP,CR-PV-I/HE} \quad (29)$$

$$CO_2^{CR-PV-I/HE} = \left(E_{el,fg}^{CR-PV-I/HE} - E_{el,tg}^{CR-PV-I/HE} \right) \times \alpha + \left(E_p^{B,CR-PV-I/HE} + E_p^{CHP,CR-PV-I/HE} \right) \times \beta \quad (30)$$

The combination of the interventions appears to have more positive effects in winter. The %E_pDR presents an average value greater than 15% in the case of CR-PV-I and equal to approximately 23% in the case of CR-PV-HE (Figures 19a and 20a).

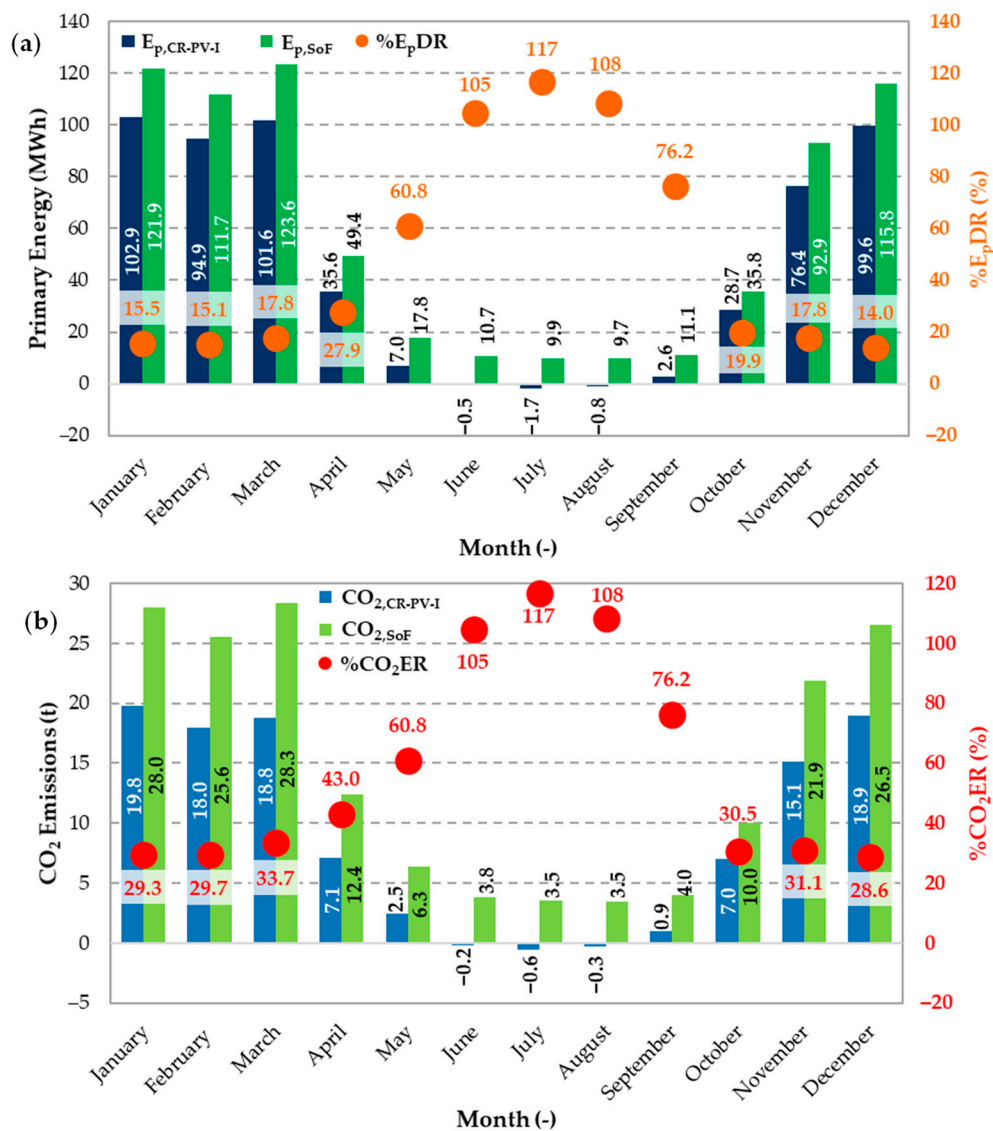


Figure 19. (a) Primary energy comparison (blue and green bars) and percentage primary energy demand reduction (orange circles), (b) CO₂ emissions (light blue and green bars) end percentage reduction (red circles) between CR-PV-I and SoF on a monthly basis.

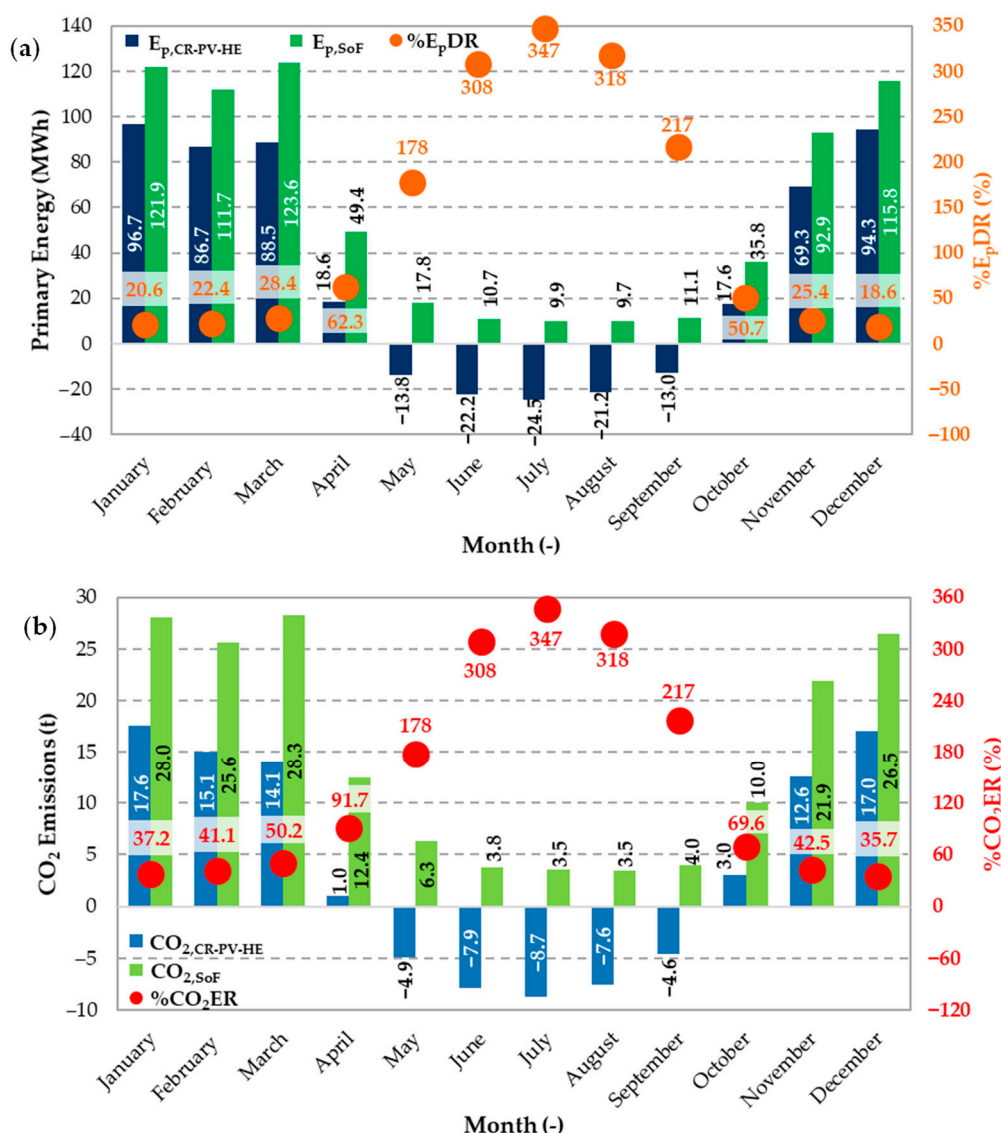


Figure 20. (a) Primary energy comparison (blue and green bars) and percentage primary energy demand reduction (orange circles), (b) CO₂ emissions (light blue and green bars) end percentage reduction (red circles) between CR-PV-HE and SoF on a monthly basis.

In the summer months from June to August the primary energy requirements is less than zero after the CR-PV-I renovation action, with a primary energy saving of 116%. In the case of CR-PV-HE the %E_pDR is greater than 100% from May to September and reaches its maximum value in July (about 350%) when a primary energy credit equal to 24.5 MWh is obtained. In terms of emissions (Figures 19b and 20b), the improvements introduced by these refurbishments are even more evident, the maximum %CO₂ER in the winter months appear in March and is equal to 33.7% for the first combined intervention and to 50% in the case of the coupling with high-performance photovoltaic panels. In the period in which the heating system is switched off there is an absolute analogy between %E_pDR and %CO₂ER as already described in the previous paragraph.

Looking at the flows of electricity (Figure 21), it is observed that in the case cogenerators and photovoltaic system are combined, the maximum amount of electricity produced and provided back to the grid ($E_{el,ig}^{CR-PV-I/HE}$) is achieved during March, when both systems contribute significantly to the on-site generation of electricity. This situation occurs in both combined interventions. In March, in addition to the large amount of electricity fed into the grid, the highest value (in absolute terms) of on-site electricity consumption is found, with the fraction of load met indexes reaching the maximum

values in both the configurations 89.5% for CR-PV-HE (solid red circle), 83.3% for CR-PV-I (empty red circle). FLM is evaluated as shown in Equation (25), considering at the numerator the electricity used on site and at the denominator both the contribution of cogenerators and photovoltaic panels. FLM in the case of the combined intervention with PV-HE is less fluctuating during the year remaining between 75 and 90% for 11 months, except for October when it is equal to around 60%. In the case of the combined intervention with PV-I, FLM in winter is observed to be high which is based basically on the cogenerators production (see Figure 15). Then it increases between June and August, due to the fact that the energy production from photovoltaic system increases also during this period. The minimum values, below 40%, take place in May and October (Figure 21, empty red circle).

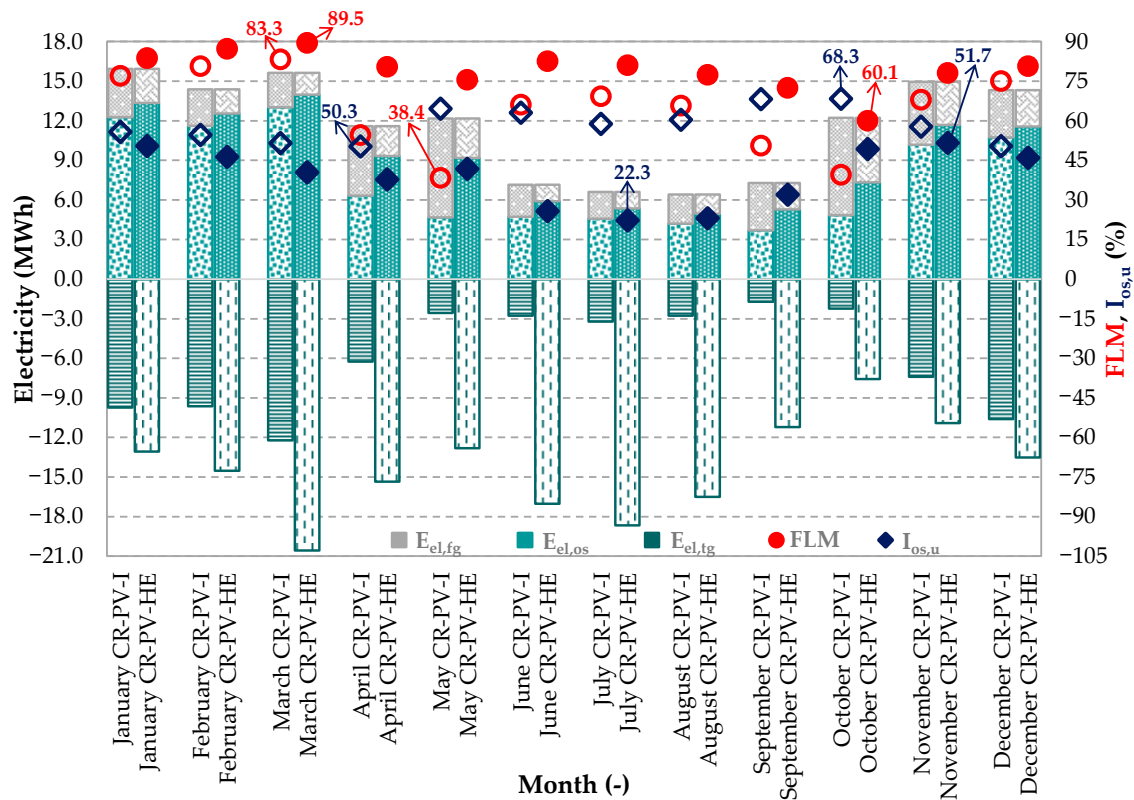


Figure 21. Electricity balance considering electricity production in the combined interventions, Fraction of Load Met (FLM) and index of on-site use ($I_{os,u}$). In each block of bars (one per month): the first stack refers to CR-PV-I, the second one to CR-PV-HE, while in each stack: the dark green textured bars represent the electric energy fed into the grid ($E_{el,tg}$), the light green textured bars the electric energy used on-site ($E_{el,os}$), the gray textured bars the electricity taken the grid ($E_{el,tg}$). Instead, the solid symbols (circle and rhombus) refer to CR-PV-HE while the empty ones to CR-PV-I.

In the analysis of the on-site use index ($I_{os,u}$), especially in the second case, it is observed that a low percentage of the electricity produced by the installed generation systems is exploited in the town hall building, while an average of about 61% is exported. This circumstance is in general not appreciable, but it mainly derives from the type of load, which is highly unbalanced towards the thermal demands, rather than towards the electrical ones and, in addition it is limited by the limited number of hours of the building occupancy. In the case of combined plants refurbishment with PV-I about 40% is exported on average.

7.6. Annual Analysis and Discussion

The energy analysis of the refurbishment interventions on an annual basis is summarized in Figure 22. For the calculation of primary energy demands and the resulting savings of each analyzed

cases with respect to SoF, the same equations reported in the monthly analysis have been applied on the annual contributions. In addition, Figure 22 highlights the rates of primary energy linked to the net electrical load (the energy drawn from the distribution grid reduced by the quantity introduced in it, $E_{p,el}$) and that related to natural gas consumption ($E_{p,NG}$).

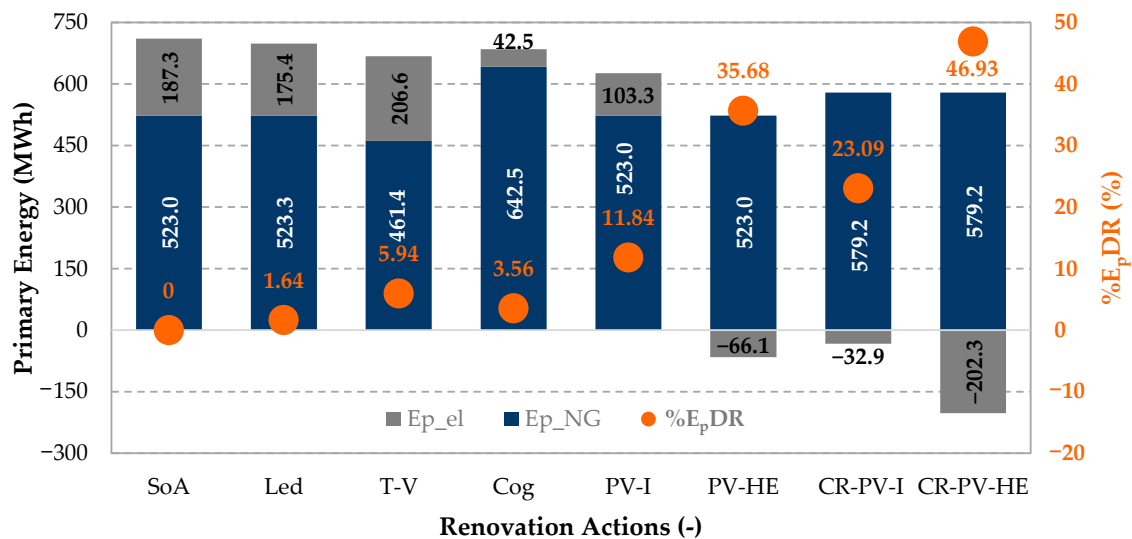


Figure 22. Energy analysis representation in terms of primary energy shares (gray and blue bars) and percentage demand reduction (orange circles) on an annual basis.

The negative values of the primary energy associated with electricity for the last three actions indicates that during a year there is a net share of electricity transferred to the national electricity grid. These negative terms are subtracted from the energy requests for natural gas to determine the total primary energy (E_p^{Act}).

Analyzing each individual intervention, it is observed that the use of thermostatic valves results to a reduction in natural gas requirements whereas the co-generators cause the increase of natural gas demand. On the contrary, with the thermostatic valves the use of electric heaters increases and therefore the related primary energy grows while the use of the cogenerating units reduces the electrical term by more than 4 times compared to the result of the SoF. The re-adaptation of the lighting system entails benefits on direct lighting energy costs but, by determining a reduction in indirect thermal contributions, it increases heating requests.

The energy advantages, represented by $\%E_pDR$, are low for all the first three cases, while the use of a renewable energy source improves these results. The most suitable solution among the two PV-based cases under examination, the PV-I intervention, allows to achieve a primary energy saving of about 12%, as it reduces electrical demands by about 45%. A high efficiency photovoltaic system significantly increases the primary energy savings; however, it faces the aesthetic problems mentioned in the initial sections. The combination of the interventions allows to obtain a $\%E_pDR = 46.9\%$ in the action providing the most efficient photovoltaic system, while, in the most appropriate combined case with PV-I the advantage reached is equal to 23.1%.

It should be emphasized in this section that by intervening only on the technical plants in the proposed case study it is possible to reduce the loads only slightly. The introduction of renewable energy sources-driven devices compensates the energy demands but does not reduce them and locally does not eliminate emissions, especially if an electrical production plant is introduced and the main requests derive from natural gas. On the other hand, the installation of a solar thermal system is difficult to manage and exploit because it would provide so much thermal energy in the summer period that must be dissipated, furthermore it would operate poorly because the terminal units present work with high temperature water.

As previously explained, without a deep plant renovation, for example by redesigning the heat transfer fluid distribution grid and the replacement of the air-conditioning system terminals, it is not possible to obtain significant results. However, environmental problems are not only local problems, the greenhouse effect must be considered at a global level and in this regard, it can be seen that the renovation choices presented can introduce significant environmental benefits (see Figure 23).

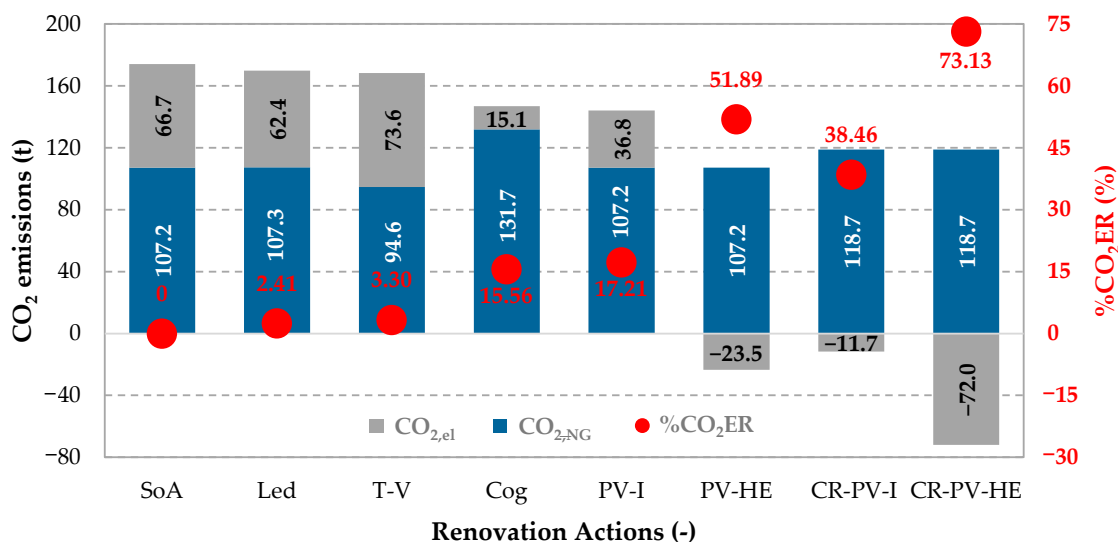


Figure 23. Environmental analysis representation in terms of CO₂ emissions shares (light blue and gray bars) and percentage emissions reduction (red circles) on an annual basis.

The combined intervention with PV-I allows an overall reduction of CO₂ emissions of 38.5% while that with high-performance panels increases the advantage to over 73%. On the base of the simulated results with the proposed interventions, it seems easier to make the town hall of Campobasso a near zero CO₂ emissions building, rather than a nearly zero energy building (nZEB). The definition of nZEB is to be intended here as a building that has energy demands on an annual basis close to zero, which, as a general principle, is in accordance with the European Directive 2010/31/EU (Energy Performance of Buildings Directive), but it doesn't follow the approach envisaged by the legislation currently in force in Italy (Interministerial Decree of 26 June 2015). The European Directive, in fact, generically defines nZEB a building that has very high energy performance where the nearly zero or very low amount of energy required should be extensively covered by renewable sources produced on-site or nearby. At European level the concept of nZEB has been introduced by the aforementioned Directive as a minimum energy performance level to be reached and then Each Member State was required to define quantitatively a range of minimum performance levels based on national conditions. The debate about the definition of nZEB is not strictly European, it involves the international technical and scientific community. Different terms are used to describe these very low energy buildings all over the world, including: zero energy building, nearly zero energy building, net zero energy, zero carbon, zero energy, zero net carbon, and zero net energy. Despite the slight difference in names, the characteristic that joins these buildings is the aim for zero-energy consumption or emissions. A further common requirement concerns the energy consumed within the building that should be for a large share derived by renewable sources, usually on-site. Finally, there are also differences on the definition of the boundary to be considered in assessing the energy balance [45]. A concept similar to that described above for nZEB is considered in this discussion for near zero CO₂ emissions building, i.e., a building that on an annual basis has an emissions balance that approach almost zero.

Still looking from a global perspective, it can be observed that although it may not reach the goal of nZEB, a public administration building can, through an effective and wise management of the territory from an energy point of view, reach and overcome the condition of zero emissions or energy

requests. Particularly, future works should focus also on examples such as the treatment of the organic fraction of the municipal solid waste, or the treatment of the wastewater from sewage discharges for the production of biomethane that could allow the elimination of fossil sources use even if it is an action done outside of the building-plant system.

Further aspects that could be analyzed in the future concern the optimization of the operation and regulation of the energy systems serving the building, more accurate assessments could also consider solutions related to the building envelope and finally optimization studies of combined solutions that also take into account economic aspects could be realized [46].

8. Conclusions

Palazzo San Giorgio is an historical building in the city of Campobasso, inner area of Southern Italy, today serving as the town hall. In this paper a series of renovation measures concerning the technical plants of the building have been studied from an energy and environmental point of view, in order to evaluate the primary energy and CO₂ emissions reductions achieved. A simulation model of the case study in the state of fact has been built with the software TRNSYS using as input the data collected in the survey campaign related to the structure, the heating system, the electric equipment, etc. The model was calibrated with respect to the billed electricity and gas consumption. Finally, simulation results of the building in its current state have been compared with those after the renovation actions. In particular, the renovation actions considered were:

- the replacement and adaptation of the lighting system with led lamps;
- the adoption of thermostatic valves for temperature regulation;
- the installation of two natural gas-powered cogenerators coupled with three thermal storage tanks;
- the introduction of an integrated photovoltaic system;
- the introduction of a high efficiency photovoltaic plant.

Excluding the installation of the photovoltaic system, the other interventions are compatible with each other and therefore, two further interventions combining the first three actions with the two photovoltaic systems have been investigated.

Two indexes have been introduced ($%E_pDR$ and $%CO_2ER$) to assess energy and environmental advantages deriving from the renovations. These indexes evaluate primary energy saving and CO₂ emission reduction in percentage terms with respect to the unmodified building-plant system. The analyses have been carried out on a monthly and annual basis and considering electricity flows to and from the national distribution grid and natural gas consumption.

The installation of the photovoltaic plants resulted in significant primary energy and emissions reductions. As far as the other retrofit actions are concerned, the energy saving was significantly lower, approximately 6% in the best case. More in detail, the cogenerators caused an increase of natural gas requirement, whereas the use of the thermostatic valves determined a reduction in natural gas requirements with respect to the state of fact. The opposite occurred for the electricity requests after these two interventions. With the cogenerating units the primary energy associated to the electricity dropped by more than four times compared to the initial results. The re-adaptation of the lighting system reduced the electric load and the indirect thermal contributions, resulting to an increase in thermal loads. Therefore, the overall contribution of the specific renovation action has been a 1.64% primary energy reduction. For all the interventions that determined a reduction in electrical demands there were more marked environmental advantages than energy benefits. The strategy of combining interventions improved the savings achieved. The most likely case involving a complete renovation with integrated photovoltaics reached a primary energy saving of 23% and avoids 38.5% of CO₂ emissions. The same indexes increased to 46.9% and 73% when the high-performance photovoltaic system has been used.

According to the simulated results of the proposed interventions, it is proved to be more feasible to make the town hall of Campobasso a near zero CO₂ emissions building, rather than a nearly zero

energy building (nZEB). Although it has not been possible with these non-invasive interventions to reach nZEB goals, however, considering the problem of climate change globally it can be said that a public administration has the possibility to reach and overcome the condition of zero emissions or zero energy requirement by means of an effective and wise management of some wastes that are potentially resources for a territory. For example, the organic fraction of the municipal solid waste and the wastewater from sewage discharges can be adopted for biomethane production through the installation of specific treatment plants.

Author Contributions: All authors have transversal expertise on the main topics of this paper, and they jointly shared the structure and aims of the manuscript. More specifically, D.P. dealt more with literature review. G.P.V. and F.T. dealt more with and building-plant system description, modeling and simulation, and M.-N.A. contributed more to the results analysis. Finally, all authors equally contributed during the writing and the critical revision of the paper. All authors have read and agreed to the published version of the manuscript.

Funding: This research received no external funding.

Acknowledgments: The authors would like to profusely thank technicians of the municipality of Campobasso for their support and the whole municipal administration for providing data and for allowing the survey campaign. A sincere thanks to Eng. Michele Iacofano for his on-field precious activities.

Conflicts of Interest: The authors declare no conflict of interest.

Nomenclature

<i>A</i>	Area (m ²)
<i>a</i>	Fraction of the fluid mass of the last cylinder remaining in the pipe
<i>C</i>	Capacity constant for the specific terminal unit
<i>CO₂</i>	CO ₂ emission (kgCO ₂)
<i>c_p</i>	Specific heat (kJ/kgK)
<i>C_v</i>	coefficient of variation of the root-mean-squared error (%)
<i>E</i>	Energy (kWh)
<i>ERR</i>	Error (%)
<i>F_a</i>	Correction factor for altitude
<i>FLM</i>	Fraction of load met index (%)
<i>F_v</i>	Correction factor for fluid velocity
<i>I</i>	Index (%)
<i>M</i>	Mass (kg)
<i>m</i>	Mass flow rate (kg/s)
<i>MBE</i>	Mean bias error (%)
<i>N</i>	Number
<i>n</i>	Capacity exponent for the specific terminal unit
<i>P</i>	Power (kW)
<i>PLR</i>	Partial load ratio
<i>RMSE</i>	Root Mean Square Error (MWh)
<i>SF</i>	Solar Fraction (%)
<i>T</i>	Temperature (K) or (°C)
<i>U</i>	Thermal transmittance (W/m ² K)
<i>%E_pDR</i>	Percentage Primary Energy Demand Reduction
<i>%CO₂ER</i>	Percentage CO ₂ Emissions Reduction
Greek symbols	
<i>η</i>	Efficiency
<i>θ</i>	Time (s) or (min) or (h)
Superscripts	
<i>Act</i>	Action for renovation
<i>ave</i>	Average
<i>B</i>	Boiler
<i>CHP</i>	Cogenerators
<i>Cog</i>	Renovation case with cogenerators

<i>EG</i>	Electric grid
<i>Led</i>	Renovation case with led
<i>meas</i>	Measured
<i>Pipe</i>	Pipeline
<i>R</i>	Radiator
<i>sim</i>	Simulated
<i>T-V</i>	Renovation case with thermostatic valves
Subscripts	
<i>air</i>	Air
<i>Comb</i>	Combustion
<i>e</i>	Environment
<i>el</i>	Electric
<i>env</i>	Envelope
<i>exh</i>	Exhaust
<i>f</i>	Fluid
<i>fg</i>	From the grid
<i>in</i>	Input
<i>loss</i>	Losses
<i>max</i>	Maximum
<i>month</i>	Month
<i>NG</i>	Natural Gas
<i>os</i>	On-site
<i>out</i>	Output
<i>p</i>	Primary
<i>pp</i>	Peak power
<i>S</i>	Surface
<i>sp</i>	Set-point
<i>tg</i>	To the grid
<i>th</i>	Thermal
<i>ts</i>	Time-step
<i>u</i>	Use
<i>year</i>	Referred to year
Acronyms	
<i>AC</i>	Alternating current
<i>CHP</i>	Combined heat and power, cogenerators
<i>Cog</i>	Renovation case with Cogenerators
<i>CR-PV-HE</i>	Combined renovation with high efficiency photovoltaic system
<i>CR-PV-I</i>	Combined renovation with integrated photovoltaic system
<i>DC</i>	Direct current
<i>Led</i>	Renovation case with led lamps
<i>NOCT</i>	Nominal operating cell temperature
<i>nZEB</i>	Nearly Zero Energy Building
<i>PV-HE</i>	Renovation case with High Efficiency photovoltaic system
<i>PV-I</i>	Renovation case with Integrated photovoltaic system
<i>SoF</i>	State of fact
<i>T-V</i>	Renovation case with thermostatic valves

Appendix A

The following Table A1 lists the monthly electricity requests for the years 2016, 2018 and 2019 divided per time slots.

Table A1. Billed electricity demand [29].

Month	Electricity Demand (kWh)								
	F1			F2			F3		
	2016	2017	2018	2016	2017	2018	2016	2017	2018
January	9190	11,379	9688	1642	1412	1750	2346	1824	2329
February	9077	8256	10,025	1554	1410	1734	1749	1595	1796
March	9968	7893	8794	1613	1654	2104	1827	2147	2424
April	6595	5779	6221	1477	1521	1574	2091	2217	2609
May	9141	7376	7427	1500	1360	1461	2173	1883	2100
June	5168	4281	4863	1212	1254	1386	2038	1866	2101
July	4514	4132	4543	1257	1333	1276	1869	1845	1992
August	4365	3692	4209	1134	1178	1393	1794	1796	2248
September	5697	4616	4628	1306	1402	1497	1782	1848	2076
October	8392	7522	8076	1477	1463	1561	1843	2116	2007
November	9241	8577	9217	1629	1630	1851	1864	1926	2481
December	8499	9825	8583	1739	1799	1811	2383	2680	3203
Total	89,847	83,328	86,274	17,540	17,416	19,398	23,759	23,743	27,366

As a supplement for the Figures 18 and 21 the following Table A2 and A3 show the numerical value of SF, FLM and $I_{os,u}$.

Table A2. Solar Fraction (SF) and Index of on-site use ($I_{os,u}$).

Month	Solar Fraction (%)		Index of On-Site Use (%)	
	PV-I	PV-HE	PV-I	PV-HE
January	13.1	31.8	80.8	67.7
February	18.8	44.9	77.4	63.7
March	26.3	57.7	77.4	57.6
April	35.5	70.4	63.5	42.1
May	37.0	72.7	64.6	41.7
June	62.5	78.0	63.0	25.8
July	65.1	76.1	58.8	22.3
August	61.1	71.9	60.4	23.1
September	46.8	67.0	68.2	32.0
October	23.3	46.2	74.0	49.4
November	15.6	39.4	80.8	69.7
December	12.0	27.6	79.1	62.8

Table A3. Fraction of Load Met (FLM) and Index of on-site use ($I_{os,u}$).

Month	Fraction of Load Met (%)		Index of On-Site Use (%)	
	CR-PV-I	CR-PV-HE	CR-PV-I	CR-PV-HE
January	77.1	83.8	55.8	50.5
February	80.7	87.3	54.6	46.4
March	83.3	89.5	51.6	40.5
April	54.6	80.5	50.3	37.8
May	38.4	75.5	64.6	41.8
June	66.1	82.6	63.0	25.8
July	69.3	81.0	58.8	22.3
August	65.8	77.5	60.4	23.1
September	50.7	72.5	68.2	32.0
October	39.5	60.1	68.3	49.3
November	68.1	78.1	57.8	51.7
December	75.0	80.8	50.3	46.1

References

1. Martínez-Molina, A.; Tort-Ausina, I.; Cho, S.; Vivancos, J.L. Energy efficiency and thermal comfort in historic buildings: A review. *Renew. Sustain. Energy Rev.* **2016**, *61*, 70–85. [CrossRef]
2. Fotopoulou, A.; Ferrante, A.; Baldini, L.; Predari, G.; Monchi, G.; Semprini, G.; Gulli, R.; Assimakopoulos, M.; Papadaki, D. An integrated system for façade additions combining safe, energy efficient and user-orientated solutions. *TEMA Technol. Eng. Mater. Archit.* **2019**, *5*, 72–81.
3. Filippi, M. Remarks on the green retrofitting of historic buildings in Italy. *Energy Build.* **2015**, *95*, 15–22. [CrossRef]
4. Assimakopoulos, M.-N.; de Masi, R.F.; Fotopoulou, A.; Papadaki, D.; Ruggiero, S.; Semprini, G.; Vanoli, G.P. Holistic approach for energy retrofit with volumetric add-ons toward nZEB target: Case study of a dormitory in Athens. *Energy Build.* **2020**, *207*, 109630. [CrossRef]
5. Papadaki, D.; Foteinis, S.; Binas, V.; Assimakopoulos, M.N.; Tsoutsos, T.; Kiriakidis, G. A life cycle assessment of PCM and VIP in warm Mediterranean climates and their introduction as a strategy to promote energy savings and mitigate carbon emissions. *AIMS Mater. Sci.* **2019**, *6*, 944–959. [CrossRef]
6. Charalambides, A.G.; Maxoulis, C.N.; Kyriacou, O.; Blakeley, E.; Frances, L.S. The impact of Energy Performance Certificates on building deep energy renovation targets. *Int. J. Sustain. Energy* **2019**, *38*, 1–12. [CrossRef]
7. Papadaki, D.; Kiriakidis, G.; Tsoutsos, T. Applications of nanotechnology in construction industry. In *Fundamentals of Nanoparticles*; Barhoum, A., Makhlof, A.S.H., Eds.; Elsevier: Amsterdam, The Netherlands, 2018; pp. 343–370.
8. Barmpareos, N.; Papadaki, D.; Karalis, M.; Fameliari, K.; Assimakopoulos, M.N. In situ measurements of energy consumption and indoor environmental quality of a pre-retrofitted student dormitory in Athens. *Energies* **2019**, *12*, 2210. [CrossRef]
9. Mazzarella, L. Energy retrofit of historic and existing buildings. the legislative and regulatory point of view. *Energy Build.* **2015**, *95*, 23–31. [CrossRef]
10. Assimakopoulos, M.; de Masi, R.F.; Papadaki, D.; Ruggiero, S.; Vanoli, G.P. Energy audit and performance optimization of a residential university building in heating dominated climates of Italian backcountry. *TEMA Technol. Eng. Mater. Archit.* **2018**, *4*, 19–33. [CrossRef]
11. D’Agostino, D.; Zangheri, P.; Castellazzi, L. Towards nearly zero energy buildings in Europe: A focus on retrofit in non-residential buildings. *Energies* **2017**, *10*, 117. [CrossRef]
12. Ferrante, A.; Fotopoulou, A.; Semprini, G.; Cantelli, D.; Ruggiero, S.; Karalis, M.; Efthymiou, C.; Papadaki, D.; Assimakopoulos, M.N. IEQ and energy improvement of existing buildings by prefabricated facade additions: The case of a student house in Athens. *IOP Conf. Ser. Mater. Sci. Eng.* **2019**, *609*, 1–6. [CrossRef]
13. Ministry of Economic Development, Ministry of the Environment and Protection of Natural Resources and the Sea, Ministry of Infrastructure and Transport. Integrated National Energy and Climate Plan. Available online: https://ec.europa.eu/energy/sites/ener/files/documents/it_final_necp_main_en.pdf (accessed on 4 September 2020).
14. National Plan for Increasing the Number of “Nearly-Zero Energy Buildings” Guidelines and Development Framework. Available online: https://ec.europa.eu/energy/sites/ener/files/documents/italy_en_version.pdf (accessed on 4 September 2020).
15. Mazzarella, L.; Pasini, M. Integration time step issue in Mediterranean Historic Building energy simulation. *Energy Procedia* **2017**, *133*, 53–67. [CrossRef]
16. Alev, Ü.; Eskola, L.; Arumägi, E.; Jokisalo, J.; Donarelli, A.; Siren, K.; Broström, T.; Kalamees, T. Renovation alternatives to improve energy performance of historic rural houses in the Baltic Sea region. *Energy Build.* **2014**, *77*, 58–66. [CrossRef]
17. Polo López, C.S.; Frontini, F. Energy efficiency and renewable solar energy integration in heritage historic buildings. *Energy Procedia* **2014**, *48*, 1493–1502. [CrossRef]
18. Magrini, A.; Franco, G. The energy performance improvement of historic buildings and their environmental sustainability assessment. *J. Cult. Herit.* **2016**, *21*, 834–841. [CrossRef]
19. Nardi, I.; de Rubeis, T.; Taddei, M.; Ambrosini, D.; Sfarra, S. The energy efficiency challenge for a historical building undergone to seismic and energy refurbishment. *Energy Procedia* **2017**, *133*, 231–242. [CrossRef]

20. Ginks, N.; Painter, B. Energy retrofit interventions in historic buildings: Exploring guidance and attitudes of conservation professionals to slim double glazing in the UK. *Energy Build.* **2017**, *149*, 391–399. [[CrossRef](#)]
21. Şahin, C.D.; Arsan, Z.D.; Tunçoku, S.S.; Broström, T.; Akkurt, G.G. A transdisciplinary approach on the energy efficient retrofitting of a historic building in the Aegean Region of Turkey. *Energy Build.* **2015**, *96*, 128–139. [[CrossRef](#)]
22. Castaldo, V.L.; Pisello, A.L.; Boarin, P.; Petrozzi, A.; Cotana, F. The experience of international sustainability protocols for retrofitting historical buildings in Italy. *Buildings* **2017**, *7*, 52. [[CrossRef](#)]
23. Milić, V.; Ekelöw, K.; Andersson, M.; Moshfegh, B. Evaluation of energy renovation strategies for 12 historic building types using LCC optimization. *Energy Build.* **2019**, *197*, 156–170. [[CrossRef](#)]
24. Bonakdar, F.; Kalagasidis, A.S.; Mahapatra, K. The implications of climate zones on the cost-optimal level and cost-effectiveness of building envelope energy renovation and space heat demand reduction. *Buildings* **2017**, *7*, 39. [[CrossRef](#)]
25. Department of Energy Federal Energy Management Program. *M&V Guidelines: Measurement and Verification for Federal Energy Projects Version 2.2*; Schiller Associates: Oakland, CA, USA, 2000.
26. Department of Energy Federal Energy Management Program. *M&V Guidelines: Measurement and Verification for Federal Energy Projects Version 4.0*; Department of Energy Federal Energy Management Program: Washington, DC, USA, 2015.
27. Roselli, R.; Sasso, M.; Tariello, F. A Wind Electric-Driven Combined Heating, Cooling, and Electricity System for an Office Building in Two Italian Cities. *Energies* **2020**, *13*, 895. [[CrossRef](#)]
28. Roselli, R.; Diglio, G.; Sasso, M.; Tariello, F. A novel energy index to assess the impact of a solar PV-based ground source heat pump on the power grid. *Renew. Energ.* **2019**, *143*, 488–500. [[CrossRef](#)]
29. Iacofano, M. Analisi energetica del palazzo San Giorgio per la connessione ad una smartgrid locale. Master's Thesis, University of Molise, Campobasso, Italy, April 2019. (In Italian).
30. TRNSYS 17, A TRaNsientSYstem Simulation Program. Available online: https://sel.me.wisc.edu/trnsys/features/t17_1_updates.pdf (accessed on 10 July 2020).
31. T.E.S.S. Component Libraries v.17.01 for TRNSYS v17.0 and the TRNSYS Simulation Studio, Parameter/Input/Output Reference Manual, Thermal Energy System Specialists, LLC. 2004. Available online: <http://www.trnsys.com/tess-libraries/> (accessed on 10 July 2020).
32. Bellia, L.; Borrelli, M.; de Masi, R.F.; Ruggiero, S.; Vanoli, G.P. University building: Energy diagnosis and refurbishment design with cost-optimal approach. Discussion about the effect of numerical modelling assumptions. *J Build. Eng.* **2018**, *18*, 1–18. [[CrossRef](#)]
33. Suszanowicz, D. Internal heat gain from different light sources in the building lighting systems. *E3S Web Conf.* **2017**, *19*, 1–5. [[CrossRef](#)]
34. Kim, H.; Park, K.; Kim, H.; Song, Y. Study on Variation of Internal Heat Gain in Office Building by Chronology. *Energies* **2018**, *11*, 1. [[CrossRef](#)]
35. Ascione, F.; Bianco, N.; de Masi, R.F.; de' Rossi, F.; Vanoli, G.P. Energy refurbishment of existing buildings through the use of phase change materials: Energy savings and indoor comfort in the cooling season. *Appl. Energy* **2014**, *113*, 990–1007. [[CrossRef](#)]
36. Technical Data Sheet of the Cogenerators. Available online: http://www.enerblu-cogeneration.com/en/product_models/301-rec2-40-g.pdf (accessed on 10 July 2020).
37. Thermal Storage Tanks Technical Data Sheet. Available online: <https://www.cordivari.com/downloads/3378/1542/Technical%20Sheet%20Puffer.pdf> (accessed on 10 July 2020).
38. Integrated Photovoltaic System Data Sheet. Available online: https://www.invent srl.it/wp-content/uploads/_mediavault/2018/05/CABRTECO2-Depliant-Techtile-Smart.pdf (accessed on 10 July 2020). (In Italian).
39. 0/26.7 kW Inverter Technical Data Sheet. Available online: https://library.e.abb.com/public/1c4e215934ee4402a002ef2f03dbf7a2/TRIO-20.0-27.6_BCD.00379_EN_Rev_L.pdf (accessed on 10 July 2020).
40. High Efficiency Photovoltaic Panels Technical Data Sheet. Available online: https://www.sunpower.com.au/sites/default/files/2019-07/max3-400-390-370-au_0.pdf (accessed on 10 July 2020).
41. 8 kW Inverter Technical Data Sheet. Available online: https://library.e.abb.com/public/a201fd491f1a14ee85257dab0035c818/TRIO-5.8_7.5_8.5-TL-OUTD-Product%20manual%20EN-RevD.pdf (accessed on 10 July 2020).
42. 5 kW Inverter Technical Data Sheet. Available online: https://library.e.abb.com/public/a4946720ed6045c886aa85c85cad06ed/PVI-10.0-12.5_BCD.00378_EN_RevG.pdf (accessed on 10 July 2020).

43. 0 kW Inverter Technical Data Sheet. Available online: https://library.e.abb.com/public/bbea91b65f5e41199b78c39c987c9aea/PVI-55.0-330.0_BCD.00381_EN_RevB.pdf (accessed on 10 July 2020).
44. 0 kW Inverter Technical Data Sheet. Available online: https://library.e.abb.com/public/4b4c04989f064be28c0ef6cfd3cc1560/TRIO-50.0_60.0_BCD.00612_IT_RevG.pdf (accessed on 10 July 2020).
45. BUILD UP, The European Portal For Energy Efficiency In Buildings. OVERVIEW | Zero-Energy Buildings: Does the Definition Influence Their Design and Implementation? Available online: <https://www.buildup.eu/en/news/overview-zero-energy-buildings-does-definition-influence-their-design-and-implementation> (accessed on 4 September 2020).
46. Rabani, M.; Madessa, H.B.; Mohseni, O.; Nord, N. Minimizing delivered energy and life cycle cost using Graphical script: An office building retrofitting case. *Appl. Energy* **2020**, *168*, 1–19. [[CrossRef](#)]



© 2020 by the authors. Licensee MDPI, Basel, Switzerland. This article is an open access article distributed under the terms and conditions of the Creative Commons Attribution (CC BY) license (<http://creativecommons.org/licenses/by/4.0/>).